Journal of Statistical Physics (2025) 192:26
https://doi.org/10.1007/s10955-025-03405-0

Non-equilibrium Phase Coexistence in Boundary-Driven Diffusive Systems

Shin-ichi Sasa[1] · **Naoko Nakagawa**[2]

Received: 9 August 2024 / Accepted: 16 January 2025 / Published online: 3 February 2025

Abstract
Liquid–gas phase coexistence in a boundary-driven diffusive system is studied by analyzing fluctuating hydrodynamics of a density field defined on a one-dimensional lattice with a space interval Λ. When an interface width ℓ is much larger than Λ, the discrete model becomes the standard fluctuating hydrodynamics, where the phase coexistence condition is given by the local equilibrium thermodynamics. In contrast, when $\ell < \Lambda$, the most probable density profile is determined by a new variational principle, where the chemical potential at the interface is found to deviate from the equilibrium coexistence chemical potential. This means that metastable states at equilibrium stably appear near the interface as the influence of the particle current. The variational function derived in the theoretical analysis is also found to be equivalent to the variational function formulated in an extended framework of thermodynamics called global thermodynamics. Finally, the validity of the theoretical result is confirmed by numerical simulations.

Keywords Phase coexistence · Out of equilibrium · Fluctuating hydrodynamics

1 Introduction

A rich variety of phenomena exhibit non-equilibrium phase coexistence, such as boiling heat transfer, pattern formation in crystal growth, and motility-induced phase separation [1–8]. Although many such impressive phenomena are dynamic and complex, a non-trivial and surprising phenomenon has been predicted in calm and simple phase coexistence out of equilibrium. One example is the quantitative prediction that, in liquid–gas coexistence under heat conduction, the temperature of the liquid–gas interface is lower than the equilibrium coexistence temperature for the pressure [9, 10], where the equilibrium phase coexistence occurs at the first-order phase transition point far from the critical point. This phenomenon

---

Communicated by Christian Maes.

✉ Shin-ichi Sasa
sasa@scphys.kyoto-u.ac.jp

Naoko Nakagawa
naoko.nakagawa.phys@vc.ibaraki.ac.jp

[1] Department of Physics, Kyoto University, Kyoto 606-8502, Japan

[2] Department of Physics, Ibaraki University, Mito 310-8512, Japan

means that metastable states at equilibrium are stabilized by a steady current even in the linear response regime.

The prediction was presented in an extended framework of thermodynamics that we call *global thermodynamics*. This framework was first proposed as a natural extension of the minimum principle of free energy with the key concept of global temperature [9]. Applying the framework to a van-der Waals fluid revealed that the temperature of the liquid–gas interface is different from the first-order transition temperature at equilibrium. Then, the formulation was carefully arranged so that quantitative predictions could be made for real materials [10]. The equivalence among different ensembles was discussed, and finally, the maximum entropy principle was formulated for enthalpy-conserving heat conduction systems [11]. The entropy defined in the formulation is found to possess a non-additive term in addition to the space integral of the local entropy density field. This formulation enables us to apply global thermodynamics to various systems.

There have been no experimental reports on the predictions of global thermodynamics. Nevertheless, it is worth mentioning that numerical simulation of the Hamiltonian Potts model in heat conduction shows results consistent with the quantitative prediction of global thermodynamics for large enough systems [12]. The singular nature of the phase coexistence has also been discussed by analyzing a mesoscopic model describing the order parameter dynamics in heat conduction [13]. However, this analysis involves some phenomenological assumptions in calculating the singular part. Furthermore, the model is too complicated to extract the microscopic mechanism of the deviation in interface temperature from the equilibrium phase coexistence temperature.

On the basis of this background, we study a simple system that exhibits non-equilibrium phase coexistence. We consider a system in which the number density field is a single dynamical variable and the density field is directly driven by a boundary condition of the chemical potential, where the temperature is given as a constant parameter of the system. The stochastic time evolution of the density field is described in terms of a discrete form of fluctuating hydrodynamics with a space interval Λ. When the width of an interface in phase coexistence ℓ is much larger than Λ, the model is equivalent to the standard fluctuating hydrodynamics [14–17]. Then, local fluctuation properties of thermodynamic quantities are described by local equilibrium distribution [18]. In contrast, when $\ell \ll \Lambda$, the local distribution may be out of equilibrium [19]. For this case, we derive the variational function that determines the most probable density profile. We then find that the chemical potential at the interface of the most probable profile deviates from the equilibrium coexistence value. This means that metastable states at equilibrium stably appear near the interface of the driven system. The formula describing the deviation takes the same form as those phenomenologically predicted by global thermodynamics. Indeed, we can derive the variational function for this system by using the method of global thermodynamics. We also confirm the validity of the theoretical calculation by numerical simulations.

The rest of this paper is organized as follows. In Sect. 2, we introduce a stochastic model we study in this paper. We then review phase coexistence conditions for equilibrium systems, and summarizes basic issues for non-equilibrium phase coexistence. In Sect. 3, we derive a variational function by analyzing the Zubarev-McLennan representation of the stationary distribution. In Sect. 4, we rewrite the variational equation as the form giving the chemical potential at the interface. In Sect. 5, we derive the variational function using the method of global thermodynamics. In Sect. 6, we show results of numerical simulations. Section 7 provides some concluding remarks.

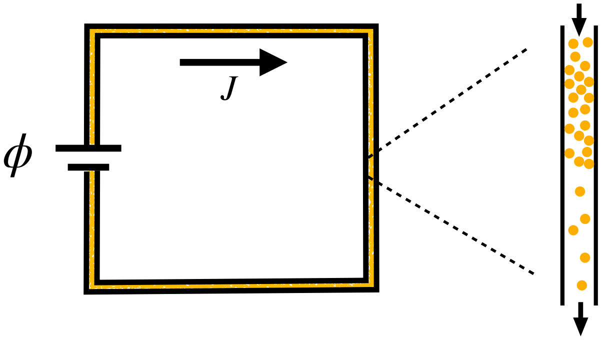

Fig. 1 Schematics of a system we study. A one-dimensional density field is defined on a ring with a battery at $x = 0$

2 Setup

2.1 Model

We consider a collection of stochastic and diffusive particles in a closed tube which are driven by an external battery at one surface $x = 0$. See Fig. 1 for the illustration of the setup. We describe the system by an averaged particle density $\rho(x)$ defined in a one-dimensional region $[0, L]$. More precisely, we define

$$\rho(x) \equiv \frac{1}{A}\int dydz\ \rho(x, y, z) \tag{2.1}$$

for the three-dimensional particle density $\rho(x, y, z)$, where the area of the cross section of the tube is denoted by A. We then assume a standard continuum description of fluctuating hydrodynamics of $\rho(x)$. The density field $\rho(x, t)$ satisfies the continuity equation

$$\partial_t \rho + \partial_x j = 0. \tag{2.2}$$

Based on the mean field picture in the cross section, we assume the current as

$$j(x, t) = -\sigma(\rho(x))\left[\partial_x \frac{\delta \mathcal{F}}{\delta \rho(x)} - \phi\delta(x)\right] + \sqrt{\frac{2\sigma(\rho(x))T}{A}} \cdot \xi(x, t). \tag{2.3}$$

T is the temperature, $\sigma(\rho)$ is a conductivity as a smooth function of ρ, and ϕ represents the voltage of a battery located at $x = 0$. ξ is Gaussian-white noise satisfying $\langle \xi \rangle = 0$ and

$$\left\langle \xi(x, t)\xi(x', t')\right\rangle = \delta(x - x')\delta(t - t'). \tag{2.4}$$

The symbol "$\cdot$" in front of ξ in (2.3) represents the Stratonovich product in space and the Ito product in time. Here, because the variance of the surface average $\Xi(x, t) \equiv \int dydz\xi(x, y, z, t)/A$ of the three-dimensional Gaussian-white noise $\xi(x, y, z, t)$ with unit variance is $1/A$, we set $\Xi(x, t) = \xi(x, t)/\sqrt{A}$, which determines the A dependence of (2.3). The free energy functional $\mathcal{F}$ of the density profile $\boldsymbol{\rho} = (\rho(x))_{0\le x\le L}$ is expressed as

$$\mathcal{F}(\boldsymbol{\rho}) = \int_0^L dx \left[f(\rho(x)) + \frac{\kappa}{2}(\partial_x \rho)^2\right]. \tag{2.5}$$

As a specific example, we consider the case that

$$f(\rho) = -\frac{1}{2}(\rho - 1.5)^2 + \frac{1}{4}(\rho - 1.5)^4 \tag{2.6}$$

by introducing dimensionless length and energy in this form. Note that our argument below is independent of the specific form if $f(\rho)$ contains two local minima. The length unit is assumed to be the order of particle distances. κ characterizes the interface free energy, which is relevant when $\partial_x \rho$ is large. In particular, when $0.5 < \bar{\rho} < 2.5$ in noiseless equilibrium systems with $T = 0$ and $\phi = 0$, phase coexistence occurs with two interfaces. Then, $\sqrt{\kappa}$ determines the interface width in the phase coexistence.

Now, we notice that there is a cutoff length Λ of the continuum description. Because the noise is assumed to be white in space, Λ should be larger than the microscopic length, which is set to the order of unity. On the other hand, it is obvious that Λ should be much smaller than the system size L. In many cases, the calculation result of fluctuating hydrodynamics is independent of the cutoff Λ even in the limit $\Lambda \to 0$, while there is a case where a singular cutoff dependence is observed [20]. Here, let us recall that the width of interfaces in phase coexistence is estimated as a microscopic length. Thus, this may be smaller than the cutoff length of fluctuating hydrodynamics. Such a case cannot be studied by the continuum model. We thus need to propose and analyze a discrete model in which the microscopic cutoff Λ is explicitly introduced.

With this background, we consider a sequence of N-boxes in a one-dimensional ring. Let ρ_i be the density of particles at the i-th box, where $1 \le i \le N$. Mathematically, ρ_i is defined on the i-th site in the one-dimensional lattice $\{i | 1 \le i \le N,\ i \in \mathbb{Z}\}$ with the periodic boundary condition $\rho_0 \equiv \rho_N$ and $\rho_{N+1} = \rho_1$. The horizontal size of the box is denoted by Λ and the cross section area of the box is A. The system size L is given by $L = \Lambda N$. The free energy functional given in (2.5) is then replaced with

$$\mathcal{F}(\boldsymbol{\rho}) = \Lambda \sum_{i=1}^{N} \left[f(\rho_i) + \frac{\kappa}{2\Lambda^2}(\rho_{i+1} - \rho_i)^2 \right] \tag{2.7}$$

for $\boldsymbol{\rho} = (\rho_i)_{1 \le i \le N}$. The density ρ_i satisfies the continuity equation

$$\frac{d\rho_i}{dt} + \frac{j_i - j_{i-1}}{\Lambda} = 0 \tag{2.8}$$

with $j_0 = j_N$. The current j_i is defined on the i-th bond connecting the i-th site and the $(i+1)$-th site. Using the generalized chemical potential $\tilde{\mu}_i$ defined by

$$\tilde{\mu}_i \equiv \frac{1}{\Lambda} \frac{\partial \mathcal{F}}{\partial \rho_i}, \tag{2.9}$$

we replace the current given in (2.3) by

$$j_i(t) = -\frac{\sigma(\rho_i^{\mathrm{m}})}{\Lambda}(\tilde{\mu}_{i+1} - \tilde{\mu}_i - \phi \delta_{i,N}) + \sqrt{\frac{2\sigma(\rho_i^{\mathrm{m}})T}{A\Lambda}} \cdot \xi_i(t), \tag{2.10}$$

where we set $\rho_i^{\mathrm{m}} = (\rho_i + \rho_{i+1})/2$ to satisfy the detailed balance condition. $\xi_i(t)$ is Gaussian-white noise satisfying $\langle \xi_i \rangle = 0$ and

$$\left\langle \xi_i(t) \xi_j(t') \right\rangle = \delta_{ij} \delta(t - t'). \tag{2.11}$$

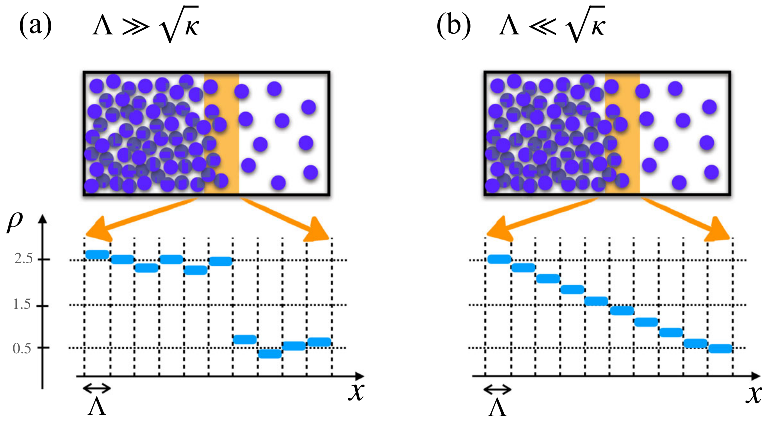

Fig. 2 Illustration of two limiting cases **a** $\kappa_\Lambda \ll 1$ and **b** $\kappa_\Lambda \gg 1$

The Λ dependence of the noise intensity in (2.10) is understood from the replacement of $\delta(x-x')$ with δ_{ij}/Λ. Explicitly, $\tilde{\mu}_i$ is written as

$$\tilde{\mu}_i = \mu(\rho_i) - \frac{\kappa}{\Lambda^2}(\rho_{i+1} + \rho_{i-1} - 2\rho_i) \tag{2.12}$$

with $\mu(\rho_i) = \partial f(\rho_i)/\partial\rho_i$. The total number of particles $\sum_{i=1}^N \rho_i = \bar{\rho}N$ is conserved in the time evolution. The average density $\bar{\rho}$ is a parameter of the system.

The steady state of this system is characterized by five parameters $(\kappa_\Lambda, T_{\rm eff}, \phi, \bar{\rho}, N)$, where

$$\kappa_\Lambda \equiv \frac{\kappa}{\Lambda^2}, \qquad T_{\rm eff} \equiv \frac{T}{A}. \tag{2.13}$$

That is, systems with the same values of $(\kappa_\Lambda, T_{\rm eff}, \phi, \bar{\rho}, N)$ exhibit the same steady state. In the argument below, the Λ dependence appear only through κ_Λ dependence. When $\kappa_\Lambda \gg 1$ and $N \to \infty$, the system behavior of (2.8) and (2.10) is understood by analyzing (2.2) and (2.3) because (2.8) and (2.10) correspond to an accurate approximation of (2.2) and (2.3). In contrast, the system behavior for the case $\kappa_\Lambda < 1$ cannot be described by (2.2) and (2.3). For such cases, we have to analyze the discrete model with focusing on the limiting case that $\kappa_\Lambda \ll 1$. See Fig. 2 for the illustration of two limiting cases. Finally, we note that $A \gg 1$ because A is the square of a macroscopic length. We thus consider the weak noise limit $T_{\rm eff} \to 0$ for the steady state realized in the limit $t \to \infty$.

2.2 Review of Equilibrium Phase Coexistence

We review phase coexistence states for the equilibrium system with $\phi = 0$. The stationary distribution of $\boldsymbol{\rho}$ is given by

$$\mathcal{P}_{\rm eq}(\boldsymbol{\rho}; \bar{\rho}) = \frac{1}{Z} \exp\left[-\frac{1}{T_{\rm eff}}\mathcal{F}(\boldsymbol{\rho})\right] \delta\left(\sum_{i=1}^N \rho_i - \bar{\rho}N\right). \tag{2.14}$$

See Appendix A for the derivation. The most probable profile in the weak noise limit $T_{\rm eff} \to 0$ is determined as the density profile that minimizes $\mathcal{F}(\boldsymbol{\rho})$ defined by (2.7). The variational

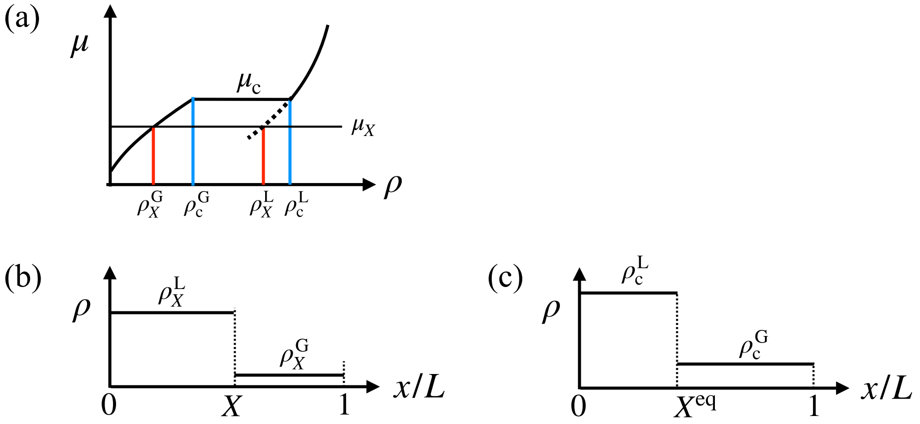

Fig. 3 **a** $\mu - \rho$ diagram. **b** and **c** represent density profiles in metastable and equilibrium states, respectively

equation is obtained as

$$\tilde{\mu}_i = \tilde{\mu}_{i+1}, \tag{2.15}$$

which means that $\tilde{\mu}_i$ is a constant independent of i.

We study two limiting cases $\kappa_\Lambda \gg 1$ and $\kappa_\Lambda \ll 1$. First, for the case $\kappa_\Lambda \gg 1$, we can derive the phase coexistence condition from the analysis of the continuum limit of (2.15) with $N \to \infty$, which is given in (B.2). Importantly, the solution of the variational equation is unique under the boundary condition that $\partial_x \rho(0) = \partial_x \rho(L) = 0$ with $\rho(0) > \rho(L)$. As shown in Appendix B, phase coexistence occurs when $\bar{\rho}$ satisfies $\rho_{\rm c}^{\rm G} \le \bar{\rho} \le \rho_{\rm c}^{\rm L}$, where $\rho_{\rm c}^{\rm L}$ and $\rho_{\rm c}^{\rm G}$ are determined by

$$\mu(\rho_{\rm c}^{\rm L}) = \mu(\rho_{\rm c}^{\rm G}), \qquad p(\rho_{\rm c}^{\rm L}) = p(\rho_{\rm c}^{\rm G}) \tag{2.16}$$

with the thermodynamic pressure $p(\rho)$ defined by

$$p(\rho) \equiv \rho\mu(\rho) - f(\rho). \tag{2.17}$$

Hereafter, the equilibrium value of the coexistence chemical potential is denoted by $\mu_c \equiv \mu(\rho_{\rm c}^{\rm L}) = \mu(\rho_{\rm c}^{\rm G})$. We assume $\rho_{\rm c}^{\rm G} < \rho_{\rm c}^{\rm L}$ without loss of generality. Then, $\rho_{\rm c}^{\rm L}$ and $\rho_{\rm c}^{\rm G}$ represent the densities of the liquid and gas in the phase coexistence, respectively. Furthermore, once $\rho_{\rm c}^{\rm L}$ and $\rho_{\rm c}^{\rm G}$ are obtained, the fraction of the liquid region $X^{\rm eq}$ is uniquely determined from $\Lambda \sum_i \rho_i = \bar{\rho}L$, which is expressed by

$$\rho_{\rm c}^{\rm L} X^{\rm eq} + \rho_{\rm c}^{\rm G}(1 - X^{\rm eq}) = \bar{\rho}. \tag{2.18}$$

See Fig. 3c for the profile.

For the other case $\kappa_\Lambda \ll 1$, which we mainly study in this paper, the derivation method in the continuum limit cannot be applied. However, even in this case, the variational principle determines the most probable profile. The variational equation (2.15) is rewritten as $\mu_i = \mu_{i+1}$ in the limit $\kappa_\Lambda \to 0$ so that the chemical potential is uniform. In this case, there is a one-parameter family of solutions $\rho_{i;X}^{\phi=0}$ characterized by $X \in [0, 1]$, where NX is a half integer. Let us write the solution $\rho_{i;X}^{\phi=0}$ explicitly. Referring to Fig. 3a, for a given X, we set $\rho_X^{\rm L}$ and $\rho_X^{\rm G}$ as those satisfying

$$\mu(\rho_X^{\rm L}) = \mu(\rho_X^{\rm G}), \qquad X\rho_X^{\rm L} + (1 - X)\rho_X^{\rm G} = \bar{\rho} \tag{2.19}$$

with $\rho_X^{\rm G} < \rho_X^{\rm L}$. We can then express the solution as

$$\rho_{i;X}^{\phi=0} = \rho_X^{\rm L}\chi(i \in [1, NX]) + \rho_X^{\rm G}\chi(i \in [NX, N]), \tag{2.20}$$

where $\chi(P)$ represents the characteristic function that takes 1 if P is true and 0 otherwise. From Fig. 3b, it is found that X corresponds to the interface position of $\rho_{i;X}^{\phi=0}$. Note that the free energy of the solutions is smaller than the other solutions with more interfaces as far as $\kappa_\Lambda > 0$. The uniform value of the chemical potential for the solution $\rho_{i;X}^{\phi=0}$ is denoted by $\mu_X^{\phi=0}$, which is equal to $\mu(\rho_X^{\rm L})$ and $\mu(\rho_X^{\rm G})$.

Note that the value of X is not determined from the variational equation (2.15) with $\kappa_\Lambda \to 0$. Physically, the solutions $\boldsymbol{\rho}_X^{\phi=0}$ form a family of metastable states characterized by X. The most probable value of X, which is denoted by X_*, is derived from the minimum free energy principle formulated as follows. We first define the variational function

$$\mathcal{F}_{\rm eq}(X; \bar{\rho}) \equiv \mathcal{F}(\boldsymbol{\rho}_X^{\phi=0}). \tag{2.21}$$

Then, the minimum free energy principle means

$$\mathcal{F}_{\rm eq}(X_*; \bar{\rho}) = \min_X \mathcal{F}_{\rm eq}(X; \bar{\rho}), \tag{2.22}$$

where, in the present case, X_* satisfies

$$\left.\frac{d\mathcal{F}_{\rm eq}(X; \bar{\rho})}{dX}\right|_{X=X_*} = 0. \tag{2.23}$$

Substituting the expression

$$\mathcal{F}(\boldsymbol{\rho}_X^{\phi=0}) = LXf(\rho_X^{\rm L}) + L(1-X)f(\rho_X^{\rm G}) \tag{2.24}$$

into (2.23), we obtain

$$f(\rho_{X_*}^{\rm L}) - f(\rho_{X_*}^{\rm G}) = \mu_{X_*}^{\phi=0}(\rho_{X_*}^{\rm L} - \rho_{X_*}^{\rm G}) \tag{2.25}$$

using (2.19) and (2.19). Comparing (2.19) and (2.25) with (2.16), we find

$$\mu_c = \mu_{X_*}^{\phi=0}, \quad \rho_{\rm c}^{\rm L} = \rho_{X_*}^{\rm L}, \qquad \rho_{\rm c}^{\rm G} = \rho_{X_*}^{\rm G}. \tag{2.26}$$

Moreover, X_* is equal to $X^{\rm eq}$. The result means that the equilibrium states for the two limiting cases, $\kappa_\Lambda \gg 1$ and $\kappa_\Lambda \ll 1$, are equivalent.

2.3 Preliminaries for Non-equilibrium Phase Coexistence

We concentrate on the case that $\bar{\rho}$ satisfies $\rho_{\rm c}^{\rm G} < \bar{\rho} < \rho_{\rm c}^{\rm L}$ where liquid and gas coexist. When the voltage of the battery ϕ is positive, the stationary distribution is not written as the canonical form (2.14). Therefore, we do not have a general variational principle for determining the most probable profile for $\phi > 0$. Nevertheless, we divide the problem for determining the most probable profile into two steps. As the first step, we consider stationary solutions of the deterministic equations without noise. If the stationary solution is unique, this is the most probable profile in the weak noise limit. In contrast, if stationary solutions form a one parameter family, we proceed to the second step, where we will formulate a variational principle for selecting the most probable profile among the stationary solutions as we have examined in (2.22) for the equilibrium system. In this section, we focus on the first step.

We consider stationary solutions of the deterministic equation given in (2.2) and (2.3) with $T_{\text{eff}} = 0$. Let J be the steady particle current induced by the battery. Setting $j_i(t) = J$ for all i in (2.3), we obtain the conduction equation

$$\frac{1}{\Lambda}\left(\tilde{\mu}_{i+1} - \tilde{\mu}_i + \phi\delta_{i,N}\right) = -\frac{J}{\sigma(\rho_i^{\mathrm{m}})}. \tag{2.27}$$

The uniformity of J yields

$$J = \phi\left(\Lambda\sum_{i=1}^{N}\frac{1}{\sigma(\rho_i^{\mathrm{m}})}\right)^{-1}. \tag{2.28}$$

When $\kappa_\Lambda \gg 1$ and $N \to \infty$ with $L = N\Lambda$ and $\kappa = \kappa_\Lambda\Lambda^2$ fixed, we can analyze the continuum limit of (2.27). As shown in Appendix B, we find that the solution of the deterministic equation is unique and that the chemical potential and pressure are continuous at the interface in the space $\hat{x} = x/L$ with $L \to \infty$. We can then conclude that the chemical potential at the interface is μ_{c}. See Appendix B for the derivation of this result.

In contrast, when we first fix $\kappa_\Lambda \ll 1$ and take the limit $N \to \infty$, there is a family of stationary solutions of the conduction equation (2.27). In the equilibrium system, they correspond to metastable states characterized by (2.19), as shown in Fig. 3b, and the metastable states were candidates for the most probable profile. We thus expect that a family of stationary solutions $\rho_{i;X}^{\phi}$ for $\phi > 0$ correspond to metastable states among which the most probable profile is selected. In the remainder of this section, we express the metastable states explicitly as a preliminary for the analysis in the next section.

We concentrate on small ϕ and ignore the contribution of $O(\phi^2)$. The solution $\rho_{i;X}^{\phi}$ should be given as a perturbation of the equilibrium solution $\rho_{i;X}^{\phi=0}$ given in (2.20). We thus assume that $|\rho_{i;X}^{\phi} - \rho_{\mathrm{c}}^{\mathrm{L}}| < |\rho_{i;X}^{\phi} - \rho_{\mathrm{c}}^{\mathrm{G}}|$ for $1 \le i < NX$, and $|\rho_{i;X}^{\phi} - \rho_{\mathrm{c}}^{\mathrm{G}}| < |\rho_{i;X}^{\phi} - \rho_{\mathrm{c}}^{\mathrm{L}}|$ for $NX < i \le N$. Letting

$$\sigma^L = \sigma(\rho_{\mathrm{c}}^{\mathrm{L}}), \qquad \sigma^G = \sigma(\rho_{\mathrm{c}}^{\mathrm{G}}), \tag{2.29}$$

the conduction equation (2.27) with $\kappa_\Lambda \to 0$ results in

$$\mu(\rho_{i;X}^{\phi}) = -\frac{1}{\sigma^L}JL\frac{i-1}{N} + \mu_{1:X}^{\phi} + O(\phi^2), \qquad (1 \le i \le NX), \tag{2.30}$$

$$\mu(\rho_{i;X}^{\phi}) = -\frac{1}{\sigma^G}JL\frac{i-N}{N} + \mu_{N;X}^{\phi} + O(\phi^2), \qquad (NX < i \le N), \tag{2.31}$$

where

$$\mu_{1;X}^{\phi} = \mu_{N;X}^{\phi} + \phi. \tag{2.32}$$

From the direct calculation, we also obtain the difference between the chemical potentials of two adjacent sites over the interface as

$$\mu(\rho_{X-1/(2N);X}^{\phi}) - \mu(\rho_{X+1/(2N);X}^{\phi}) = O(\phi/N). \tag{2.33}$$

Finally, the condition

$$\frac{1}{N}\sum_{i=1}^{N}\rho_{i;X}^{\phi} = \bar{\rho} \tag{2.34}$$

uniquely determines $\mu_{1;X}^{\phi}$ and $\rho_{1;X}^{\phi}$ for a given X. We can easily confirm that $\lim_{\phi\to 0}\rho_{i;X}^{\phi}$ is equivalent to (2.20).

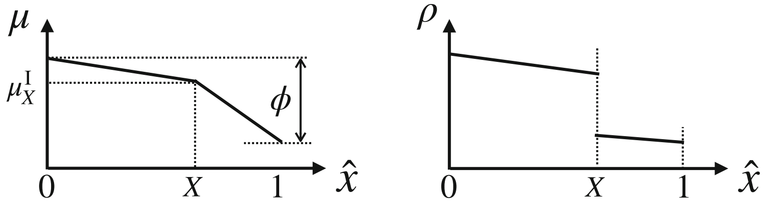

Fig. 4 Schematic profiles of $\mu_X^{\phi}(\hat{x})$ and $\rho_X^{\phi}(\hat{x})$

2.4 Singular Continuum Description

We introduce a continuum description using a real variable $\hat{x} = x/L$ defined on the interval [0, 1] by taking the limit $N \to \infty$. The mathematical formulation of this limit is beyond the scope of the present paper. However, to simplify the calculation in the subsequent sections, we naively introduce the continuum description based on expected behaviors of $\rho_i(t)$ for large N. For a discrete variable $\boldsymbol{\rho} = (\rho_i(t))_{i=1}^N$ at time t, we first define $\rho_N(\hat{x}, \hat{t})$ as the piece-wise linear function obtained by connecting two consecutive points $(i/N, \rho_i(t))$ and $((i+1)/N, \rho_{i+1}(t))$ for $0 \le i \le N$ in the $(\hat{x}, \rho)$ space, where we set $\hat{t} = t/L^2$ for later convenience. For sufficiently large N, we expect that there exists an almost continuous function $\rho(\hat{x}, \hat{t})$ such that $|\rho(\hat{x}, \hat{t}) - \rho_N(\hat{x}, \hat{t})| = O(1/N)$. The chemical potential $\mu(\hat{x}, \hat{t})$ in the continuum description is defined from $\mu_i(t)$ by the same procedure and it is expected that $\mu(\hat{x}, \hat{t}) = \mu(\rho(\hat{x}, \hat{t}))$. The definition of $j(\hat{x}, \hat{t})$ is slightly different from $\rho(\hat{x}, \hat{t})$ and $\mu(\hat{x}, \hat{t})$, because the current $j_i(t)$ is defined on the i-th bond connecting the i site and $i+1$ site as seen in (2.8) and (2.10). Concretely, we define $j(\hat{x}, \hat{t})$ by using the piece-wise linear function obtained by connecting points $(i/N + 1/2N, j_i/L)$ in the $(\hat{x}, j)$ space. Then, the continuum limit of (2.8) and (2.10) with $\kappa_\Lambda \to 0$ is expressed by

$$\partial_{\hat{t}} \rho(\hat{x}, \hat{t}) + \partial_{\hat{x}} j(\hat{x}, \hat{t}) = 0, \tag{2.35}$$

and

$$j(\hat{x}, \hat{t}) = -\sigma(\rho(\hat{x}, \hat{t})) \left[\frac{\partial \mu(\hat{x}, \hat{t})}{\partial \hat{x}} - \phi \delta(\hat{x}) \right] + \sqrt{\frac{2\sigma(\rho(\hat{x}, \hat{t})) T_{\mathrm{eff}}}{L}} \cdot \hat{\xi}(\hat{x}, \hat{t}), \tag{2.36}$$

where $\hat{\xi}(\hat{x}, \hat{t})$ satisfies

$$\left\langle \hat{\xi}(\hat{x}, \hat{t}) \hat{\xi}(\hat{x}', \hat{t}') \right\rangle = \delta(\hat{x} - \hat{x}') \delta(\hat{t} - \hat{t}'). \tag{2.37}$$

Apparently, (2.35) and (2.36), which we call *the singular continuum description*, take the same form as a singular case of the standard continuum description (2.2) and (2.3) with $\kappa \to 0$ by setting $\hat{x} = x/L$ and $\hat{t} = t/L^2$. We here notice the difference between the two descriptions. In the singular continuum description, we first take $N \to \infty$ with L and κ_Λ fixed, and then consider $\kappa_\Lambda \to 0$. On the other hand, as described in the previous subsection, in the standard continuum description, we take $\kappa_\Lambda = \kappa/\Lambda^2 \to \infty$ and $N \to \infty$ with L and κ fixed. Then, as a singular case of the standard continuum description, we consider the limit $\kappa \to 0$. The behavior of the two descriptions are rather different, but we do not discuss the difference anymore. In the argument below, we will consider only the singular continuum description.

The stationary solution of the deterministic equation $\rho_{i;X}^{\phi}$ and the corresponding chemical potential $\mu(\rho_{i;X}^{\phi})$ are expressed as $\rho_X^{\phi}(\hat{x})$ and $\mu_X^{\phi}(\hat{x})$ in the singular continuum description.

Note that $\rho_X^\phi(\hat{x})$ is discontinuous at $\hat{x} = X$, while $\mu_X^\phi(\hat{x})$ is continuous at $\hat{x} = X$ as is seen from (2.33). The chemical potential at the interface $\hat{x} = X$ is denoted by

$$\mu_X^{\mathrm{I}} \equiv \mu_X^\phi(X). \tag{2.38}$$

As shown in Fig. 4, $\rho_X^\phi(\hat{x})$ is a piece-wise continuous function and that $\mu_X^\phi(\hat{x})$ is a piece-wise smooth function with singular points at $\hat{x} = 0$ and $\hat{x} = X$. Furthermore, we rewrite (2.30) and (2.32) as

$$\mu_X^\phi(\hat{x}) = -\frac{1}{\sigma^L} JL\hat{x} + \mu_X^\phi(0) + O(\phi^2) \tag{2.39}$$

for $0 \le \hat{x} < X$, and

$$\mu_X^\phi(\hat{x}) = -\frac{1}{\sigma^G} JL(\hat{x} - 1) + \mu_X^\phi(1) + O(\phi^2) \tag{2.40}$$

for $X < \hat{x} \le 1$. We also have

$$\mu_X^\phi(0) = \mu_X^\phi(1) + \phi. \tag{2.41}$$

Here, from (2.28), we obtain

$$JL = \phi\left(\frac{X}{\sigma^{\mathrm{L}}} + \frac{1 - X}{\sigma^{\mathrm{G}}}\right)^{-1}. \tag{2.42}$$

Then, the density field $\rho_X^\phi(\hat{x})$ for $0 \le \hat{x} < X$ is determined from (2.39) with $\mu_X^\phi(\hat{x}) = \mu(\rho_X^\phi(\hat{x}))$ and $|\rho_X^\phi(\hat{x}) - \rho_{\mathrm{c}}^{\mathrm{L}}| < |\rho_X^\phi(\hat{x}) - \rho_{\mathrm{c}}^{\mathrm{G}}|$. Similarly, the density field $\rho_X^\phi(\hat{x})$ for $X < \hat{x} \le 1$ is determined from (2.40) with $\mu_X^\phi(\hat{x}) = \mu(\rho_X^\phi(\hat{x}))$ and $|\rho_X^\phi(\hat{x}) - \rho_{\mathrm{c}}^{\mathrm{G}}| < |\rho_X^\phi(\hat{x}) - \rho_{\mathrm{c}}^{\mathrm{L}}|$. Note that $\rho_X^\phi(\hat{x})$ and $\partial_{\hat{x}}\mu_X^\phi(\hat{x})$ are discontinuous at $\hat{x} = 0$ and $\hat{x} = X$. For given X and system parameters $(\phi, \bar{\rho})$, $\mu_X^\phi(\hat{x})$ and $\rho_X^\phi(\hat{x})$ are uniquely determined from the condition

$$\int_0^1 d\hat{x}\ \rho_X^\phi(\hat{x}) = \bar{\rho}. \tag{2.43}$$

3 Variational Function

To simplify the notation, we use x and t for $\hat{x}$ and $\hat{t}$ in this and next sections. In the previous section, we determined the candidates of steady density profile $\rho_X^\phi(x)$ characterized by X in the weak noise limit $T_{\mathrm{eff}} \to 0$. To determine the most probable density profile among them for given system parameters $(\bar{\rho}, \phi)$, in Sect. 3.1, we derive a variational function using the Zubarev-McLennan representation of the steady state. The variational function includes a time integral of the current at $x = 0$. After confirming some basic issues and assumptions in Sect. 3.2, we calculate the time integral of the current in Sect. 3.3. The result is presented in Sect. 3.4.

3.1 Stationary Distribution

We consider the stationary distribution $\mathcal{P}_{\mathrm{ss}}(\boldsymbol{\rho}; \bar{\rho}, \phi)$ of density field $\boldsymbol{\rho}$. When $\phi = 0$, the stationary distribution is given by (2.14). However, the stationary distribution for the system with $\phi > 0$ is not generally obtained. Nevertheless, in the linear response regime out of

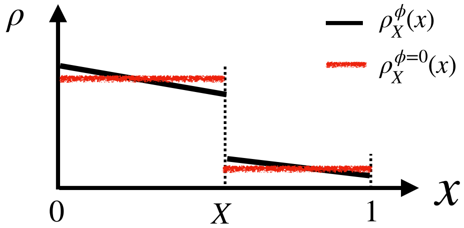

Fig. 5 Schematic relationship between $\rho_X^{\phi}(x)$ and $\rho_X^{\phi=0}(x)$

equilibrium, there is a useful expression called the Zubarev-McLennan representation

$$\mathcal{P}_{\rm ss}(\boldsymbol{\rho};\bar\rho,\phi)=\mathcal{P}_{\rm eq}(\boldsymbol{\rho};\bar\rho)\exp\left[-\frac{\phi\,\langle Q\rangle_{\boldsymbol{\rho}}^{\rm eq}+O(\phi^2)}{T_{\rm eff}}\right] \tag{3.1}$$

with

$$Q=\int_0^\infty dt\ j_N(t), \tag{3.2}$$

where $j_N(t)$ is a fluctuating current at the N-th bond, which is defined in (2.10). The N-th bond is the only bond on which the driving ϕ is imposed. $\langle\ \rangle_{\boldsymbol{\rho}}^{\rm eq}$ denotes the conditioned expectation for the equilibrium path ensemble provided that the initial density profile is given by the specified $\boldsymbol{\rho}$ as the argument of the stationary distribution [21–27]. See Appendix C for the derivation of (3.1).

For the general expression (3.1) with (3.2), we take the limit $\kappa_\Lambda\to 0$ and consider the singular continuum description introduced in the previous section. From (2.14) and (3.1), we have

$$\mathcal{P}_{\rm ss}(\boldsymbol{\rho};\bar\rho,\phi)=\exp\left[-\frac{1}{T_{\rm eff}}(\mathcal{F}(\boldsymbol{\rho})+\phi\,\langle Q\rangle_{\boldsymbol{\rho}}^{\rm eq}+O(\phi^2)+{\rm const})\right]\delta\left(\int_0^1 dx\,\rho(x)-\bar\rho\right) \tag{3.3}$$

with

$$Q=L\int_0^\infty dt\ j(0,t). \tag{3.4}$$

Note that $j_N(t)$ becomes $j(0,t)=j(1,t)$ in the singular continuum description. The most probable density profile is identified as $\rho_{X_*}^{\phi}(x)$ that minimizes $-\log\mathcal{P}_{\rm ss}(\boldsymbol{\rho}_X^{\phi};\bar\rho,\phi)$. This is the variational principle to determine X_*. From (3.3), we obtain the variational function as

$$\mathcal{F}_{\rm ss}(X;\bar\rho,\phi)=\mathcal{F}(\boldsymbol{\rho}_X^{\phi})+\phi\,\langle Q\rangle_{\boldsymbol{\rho}_X^{\phi}}^{\rm eq}+O(\phi^2). \tag{3.5}$$

We then find X_* as the special value of X that minimizes the variational function $\mathcal{F}_{\rm ss}(X;\bar\rho,\phi)$ with $(\bar\rho,\phi)$ fixed. That is, X_* is determined as

$$\mathcal{F}_{\rm ss}(X_*;\bar\rho,\phi)=\min_X\mathcal{F}_{\rm ss}(X;\bar\rho,\phi). \tag{3.6}$$

We thus need to calculate $\langle Q\rangle_{\boldsymbol{\rho}_X^{\phi}}^{\rm eq}$.

3.2 Preliminaries for the Calculation $\langle Q\rangle^{\mathrm{eq}}_{\rho_X^\phi}$

To calculate $\langle Q\rangle^{\mathrm{eq}}_{\rho_X^\phi}$, we have to know the typical time evolution of $\rho(x,t)$ starting from $\rho_X^\phi(x)$ at $t=0$ under the equilibrium condition $\phi=0$ in the weak noise limit $T_{\mathrm{eff}}\to 0$, where $T_{\mathrm{eff}}\to 0$ is taken after $t\to\infty$ is considered. Here, from (3.5), we find that only ϕ-independent terms of $\langle Q\rangle^{\mathrm{eq}}_{\rho_X^\phi}$ are necessary for the calculation because ϕ-dependent terms are absorbed into $O(\phi^2)$. We then notice expansions

$$\mu_X^\phi(x)=\mu_X^{\phi=0}(x)+O(\phi),\qquad \rho_X^\phi(x)=\rho_X^{\phi=0}(x)+O(\phi). \tag{3.7}$$

See Fig. 5 for illustration of $\rho_X^\phi(x)$ and $\rho_X^{\phi=0}(x)$. See also the sentence involving (2.19) for $\mu_X^{\phi=0}$. Using these relations, we find

$$\langle Q\rangle^{\mathrm{eq}}_{\rho_X^\phi}=\langle Q\rangle^{\mathrm{eq}}_{\rho_X^{\phi=0}}+O(\phi). \tag{3.8}$$

That is, we study the typical time evolution of the density field starting from $\rho_X^{\phi=0}(x)$. Since we study the case $\kappa_\Lambda\to 0$, $\rho_X^{\phi=0}(x)$ represents a metastable profile that does not evolve in time without noises. Nevertheless, weak noise slowly drives the metastable profile $\rho_X^{\phi=0}(x)$ to the equilibrium state characterized by (2.14). One may conjecture that the most probable time evolution from $\rho_X^{\phi=0}(x)$ in the weak noise limit is described by the relaxation process to the equilibrium profile $\rho_{X_*}^{\phi=0}(x)$ in Fig. 3c from the metastable profile in Fig. 3b. However, this is not correct because of the space translational symmetry of equilibrium systems. Note that metastable profiles for a given width X of the liquid region form a one-parameter family of profiles obtained by any space translation of $\rho_X^{\phi=0}(x)$, and similarly equilibrium profiles also form a one-parameter family. Thus, stochastic dynamics in this neutral direction are equally probable, which are represented by Brownian motion of the profile with the width of the liquid region fixed. In other words, most probable process is not uniquely determined in the weak noise limit. We have to consider a collection of trajectories that are equally probable and dominantly contribute to $\langle Q\rangle^{\mathrm{eq}}_{\rho_X^{\phi=0}}$. We call this collection *the highly probable path ensemble* to distinguish it with the most probable process.

Here, we concretely describe the highly probable path ensemble starting from the initial condition $\rho_X^{\phi=0}(x)$. We assume that each trajectory in the highly probable path ensemble satisfies the following two conditions. First, the liquid or gas region is not separated into smaller pieces of liquid or gas at any time t. That is, the number of interfaces in the system is always two. Second, slow dynamics occurs along a continuous family of metastable states by the influence of weak noise, where the metastable states are characterized by the position of two interfaces. We then consider the time evolution $\rho(x,t)$ as follows. Let $D^{\mathrm{L}}(t)$ and $D^{\mathrm{G}}(t)$ denote the liquid region and gas region at any time t. Recalling the relation (2.20) with (2.19), we express $\rho(x,t)$ in the highly probable path ensemble as

$$\rho(x,t)=\rho^{\mathrm{L}}(t)\chi(x\in D^{\mathrm{L}}(t))+\rho^{\mathrm{G}}(t)\chi(x\in D^{\mathrm{G}}(t)), \tag{3.9}$$

where $\rho^{\mathrm{L}}(t)$ and $\rho^{\mathrm{G}}(t)$ are determined from

$$\mu(\rho^{\mathrm{L}}(t))=\mu(\rho^{\mathrm{G}}(t)) \tag{3.10}$$

and

$$\rho^{\mathrm{L}}(t)|D^{\mathrm{L}}(t)|+\rho^{\mathrm{G}}(t)|D^{\mathrm{G}}(t)|=\bar{\rho}. \tag{3.11}$$

It should be noted that we adopt the singular continuum description introduced in the previous section. Using this form of the time evolution, we estimate (3.2).

Because $\rho(x,t)$ in (3.9) is described by $D^{\mathrm{L}}(t)$ and $D^{\mathrm{G}}(t)$, we explicitly express them in terms of the interface positions $X_{\uparrow}(t)$ and $X_{\downarrow}(t)$ at time t, where they satisfy

$$\rho(X_{\uparrow}(t)+\epsilon,t)-\rho(X_{\uparrow}(t)-\epsilon,t)>0,\quad \rho(X_{\downarrow}(t)+\epsilon,t)-\rho(X_{\downarrow}(t)-\epsilon,t)<0 \tag{3.12}$$

for small positive ϵ. See Fig. 6a. Then, the liquid region $D^{\mathrm{L}}(t)$ and gas region $D^{\mathrm{G}}(t)$ are expressed as $D^{\mathrm{L}}(t)=[X_{\uparrow}(t),X_{\downarrow}(t)]$ and $D^{\mathrm{G}}(t)=[0,1]\backslash D^{\mathrm{L}}(t)$ if $X_{\uparrow}(t)<X_{\downarrow}(t)$, or $D^{\mathrm{G}}(t)=[X_{\downarrow}(t),X_{\uparrow}(t)]$ and $D^{\mathrm{L}}(t)=[0,1]\backslash D^{\mathrm{G}}(t)$ if $X_{\uparrow}(t)>X_{\downarrow}(t)$.

Now, we consider the time evolution of interface positions, $X_{\uparrow}(t)$ and $X_{\downarrow}(t)$, starting from $X_{\uparrow}(0)=0$ and $X_{\downarrow}(0)=X$. However, because $0\le X_{\uparrow}(t)\le 1$ and $0\le X_{\downarrow}(t)\le 1$, $X_{\uparrow}(t)$ and $X_{\downarrow}(t)$ are not continuous functions of t. This would lead to a complicated calculation of the accumulated current defined by (3.4). To describe the interface motion using continuous functions, we introduce generalized coordinates $\hat{X}_{\uparrow}(t)\in\mathbb{R}$ and $\hat{X}_{\downarrow}(t)\in\mathbb{R}$ such that displacements of the interface from the initial time 0 to the time t are given by $\hat{X}_{\uparrow}(t)-\hat{X}_{\uparrow}(0)$ and $\hat{X}_{\downarrow}(t)-\hat{X}_{\downarrow}(0)$. That is, $\hat{X}_{\uparrow}(t)$ and $\hat{X}_{\downarrow}(t)$ describe the positions of the left and right interfaces of the liquid region in a generalized coordinate space $\mathbb{R}$. The interface positions $X_{\uparrow}(t)$ and $X_{\downarrow}(t)$ in the space $[0,1]$ are then obtained as

$$X_{\uparrow}(t)=\hat{X}_{\uparrow}(t)-\lfloor\hat{X}_{\uparrow}(t)\rfloor,\qquad X_{\downarrow}(t)=\hat{X}_{\downarrow}(t)-\lfloor\hat{X}_{\downarrow}(t)\rfloor, \tag{3.13}$$

where $\lfloor\ \rfloor$ represents the floor function. The width of the liquid and gas regions are then written as

$$|D^{\mathrm{L}}(t)|=\hat{X}_{\downarrow}(t)-\hat{X}_{\uparrow}(t),\quad |D^{\mathrm{G}}(t)|=1-|D^{\mathrm{L}}(t)|=\hat{X}_{\uparrow}(t)-\hat{X}_{\downarrow}(t)+1 \tag{3.14}$$

irrespective of the sign of $X_{\downarrow}(t)-X_{\uparrow}(t)$. We also introduce the center of the liquid region in the generalized coordinate space as

$$\hat{Y}(t)=\frac{\hat{X}_{\uparrow}(t)+\hat{X}_{\downarrow}(t)}{2}. \tag{3.15}$$

Using the width $|D^{\mathrm{L}}(t)|$ and the center $\hat{Y}(t)$ of the liquid region, we have

$$\hat{X}_{\downarrow}(t)=\hat{Y}(t)+\frac{|D^{\mathrm{L}}(t)|}{2},\qquad \hat{X}_{\uparrow}(t)=\hat{Y}(t)-\frac{|D^{\mathrm{L}}(t)|}{2}. \tag{3.16}$$

We note that, in the weak noise limit, $|D^{\mathrm{L}}(t)|$ obeys a deterministic equation describing $|D^{\mathrm{L}}(t)|\to X^{\mathrm{eq}}$ as $t\to\infty$, while $\hat{Y}(t)$ shows unbounded-free Brownian motion because of the translation symmetry for the case $\phi=0$. This fact simplifies the calculation of the accumulated current defined by (3.2).

At the end of this subsection, we discuss the difference between the most probable process for the case $\kappa_{\Lambda}\gg 1$ and the highly probable path ensemble for the case $\kappa_{\Lambda}\ll 1$. In the former case, $\rho_X^{\phi=0}$ evolves to an equilibrium configuration in the deterministic system, which is in contrast with the latter case. To obtain the accumulated current Q for the former case, we have to analyze the time-dependent solution of the deterministic equation, which is out of the present paper.

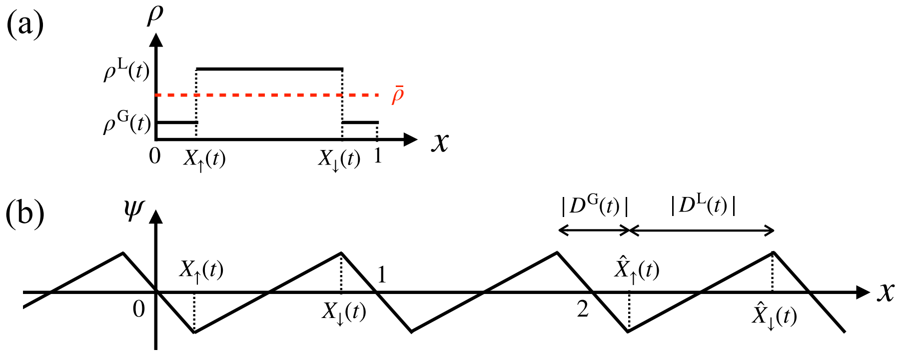

Fig. 6 **a** Density profile $\rho(x,t)$ whose interface positions are $X_\uparrow(t)$ and $X_\downarrow(t)$. $\rho(x,t)=\rho^{\mathrm{L}}(t)$ in $D^{\mathrm{L}}(t)=[X_\uparrow(t),X_\downarrow(t)]$, while $\rho(x,t)=\rho^{\mathrm{G}}(t)$ in $D^{\mathrm{G}}(t)=[0,1]\backslash D^{\mathrm{L}}(t)$. **b** Example of $\psi(x,t)$ defined in $-\infty<x<\infty$

3.3 Expression of $j(0,t)$

In this subsection, we calculate $j(x,t)$ in the singular continuum description based on (2.35) and (2.36). In the argument below, $\hat{X}_\uparrow(t)$, $\hat{X}_\downarrow(t)$, $D^{\mathrm{L}}(t)$, and $D^{\mathrm{G}}(t)$ are simply denoted by $\hat{X}_\uparrow$, $\hat{X}_\downarrow$, D^{L}, and D^{G} if their t-dependencies are clearly guessed.

For a given density profile $(\rho(x,t))_{x=0}^{1}$ at time t, we define

$$\psi(x,t)\equiv\int_0^x dx'(\rho(x',t)-\bar{\rho}) \tag{3.17}$$

for $0\le x\le 1$. Because $\psi(0,t)=\psi(1,t)=0$, $\psi(x,t)$ can be extended to a periodic function in x. That is, we define $\psi(x,t)\equiv\psi(x-\lfloor x\rfloor,t)$ for any $-\infty<x<\infty$. See Fig. 6b for the illustration. The time derivative of (3.17) leads to

$$\partial_t\psi(x,t)=-j(x,t)+j(0,t) \tag{3.18}$$

for any $x\in[0,1]$. We here integrate (3.18) over the liquid region and divide by σ^{L}. We repeat the same operation for the gas region. Summing up the two results, we have a relation

$$\begin{aligned}&\frac{1}{\sigma^{\mathrm{L}}}\int_{D^{\mathrm{L}}}dx\,\partial_t\psi+\frac{1}{\sigma^{\mathrm{G}}}\int_{D^{\mathrm{G}}}dx\,\partial_t\psi\\&=-\frac{1}{\sigma^{\mathrm{L}}}\int_{D^{\mathrm{L}}}dx\,j(x,t)-\frac{1}{\sigma^{\mathrm{G}}}\int_{D^{\mathrm{G}}}dx\,j(x,t)+\left(\frac{|D^{\mathrm{L}}|}{\sigma^{\mathrm{L}}}+\frac{|D^{\mathrm{G}}|}{\sigma^{\mathrm{G}}}\right)j(0,t).\end{aligned} \tag{3.19}$$

Here, we attempt to extract slow dynamics of $j(0,t)$ by considering a short-time average of (3.19). Recalling the formula for $j(x,t)$ given in (2.36), we find that, in the weak noise limit, $\mu(x,t)$ takes a constant value in the bulk regions and the space integral of the noise term is estimated as zero by the short-time average. Then, the first and second terms on the right side of (3.19) turn out to be zero. We thus obtain the expression for $j(0,t)$ as

$$j(0,t)=\left[\frac{|D^{\mathrm{L}}|}{\sigma^{\mathrm{L}}}+\frac{|D^{\mathrm{G}}|}{\sigma^{\mathrm{G}}}\right]^{-1}\left[\frac{1}{\sigma^{\mathrm{L}}}\int_{D^{\mathrm{L}}}dx\ \partial_t\psi+\frac{1}{\sigma^{\mathrm{G}}}\int_{D^{\mathrm{G}}}dx\ \partial_t\psi\right]. \tag{3.20}$$

We remark that $j(0,t)$ is still stochastic. Indeed, in the right side of (3.20), $D^{\mathrm{L}}(t)$, $D^{\mathrm{G}}(t)$, and the space integrals of $\partial_t\psi(x,t)$ are affected by the Brownian motion of the interfaces.

The current $j(0,t)$ formulated in (3.20) contains the time derivative of ψ in the space integrals. We now transform (3.20) into a formula by letting the time derivative be outside the integral. In the transformation procedure, we need to pay attention to the time-dependent ranges D^{L} and D^{G} of the integrals. As the result, the current $j(0,t)$ is expressed as

$$j(0,t) = \Phi(t) - \Phi_0(t), \tag{3.21}$$

where

$$\Phi(t) \equiv \frac{d}{dt}\left\{\left[\frac{|D^{\mathrm{L}}|}{\sigma^{\mathrm{L}}} + \frac{|D^{\mathrm{G}}|}{\sigma^{\mathrm{G}}}\right]^{-1}\left[\frac{1}{\sigma^{\mathrm{L}}}\int_{D^{\mathrm{L}}} dx\,\psi + \frac{1}{\sigma^{\mathrm{G}}}\int_{D^{\mathrm{G}}} dx\,\psi\right]\right\}, \tag{3.22}$$

and $\Phi_0(t)$ is determined from (3.20), (3.21), and (3.22). Concretely, we perform the time-derivative of (3.22). In the time derivative of a function of Brownian motion $X(t)$, we note the chain rule $df(X(t))/dt = f'(X(t)) \circ dX/dt$, where the symbol $\circ$ represents the Stratonovich product. We then have

$$\Phi_0(t) = \left(\frac{1}{\sigma^{\mathrm{L}}} - \frac{1}{\sigma^{\mathrm{G}}}\right)\left[\frac{|D^{\mathrm{L}}(t)|}{\sigma^{\mathrm{L}}} + \frac{|D^{\mathrm{G}}(t)|}{\sigma^{\mathrm{G}}}\right]^{-1} |D^{\mathrm{L}}(t)|(\rho^{\mathrm{L}}(t) - \bar{\rho}) \circ \frac{d}{dt}\hat{Y}. \tag{3.23}$$

See Appendix D for the derivation of $\Phi_0(t)$.

Due to the translational invariance for the case $\phi = 0$, $\hat{Y}(t)$ shows the free Brownian motion. Because $|D^{\mathrm{L}}(t)|$ and $\rho^{\mathrm{L}}(t)$ obey deterministic equations in the weak noise limit, they have no correlation with $\hat{Y}(t)$. Therefore, taking the path ensemble average over noise realization, we have

$$\begin{aligned}\langle \Phi_0(t)\rangle &= \left(\frac{1}{\sigma^{\mathrm{L}}} - \frac{1}{\sigma^{\mathrm{G}}}\right)\left\langle\left[\frac{|D^{\mathrm{L}}(t)|}{\sigma^{\mathrm{L}}} + \frac{|D^{\mathrm{G}}(t)|}{\sigma^{\mathrm{G}}}\right]^{-1} |D^{\mathrm{L}}(t)|(\rho^{\mathrm{L}}(t) - \bar{\rho})\right\rangle\left\langle\frac{d}{dt}\hat{Y}\right\rangle \\ &= 0\end{aligned} \tag{3.24}$$

Combining this with (3.21), we obtain

$$\langle j(0,t)\rangle^{\mathrm{eq}}_{\rho_X^{\phi=0}} = \langle \Phi(t)\rangle^{\mathrm{eq}}_{\rho_X^{\phi=0}}\,. \tag{3.25}$$

3.4 Result of $\langle Q\rangle^{\mathrm{eq}}_{\rho_X^{\phi=0}}$

Let us define

$$q(\tau) \equiv \int_0^{\tau} dt\,\Phi(t). \tag{3.26}$$

From (3.4) and (3.25), we have

$$\langle Q\rangle^{\mathrm{eq}}_{\rho_X^{\phi=0}} = L \lim_{\tau\to\infty} \langle q(\tau)\rangle^{\mathrm{eq}}_{\rho_X^{\phi=0}}\,. \tag{3.27}$$

Substituting (3.22) into (3.26) with noting $X_{\uparrow}(0) = 0$ and $X_{\downarrow}(0) = X$, we obtain

$$\begin{aligned} q(\tau) =& \left[\frac{|D^{\mathrm{L}}(\tau)|}{\sigma^{\mathrm{L}}} + \frac{|D^{\mathrm{G}}(\tau)|}{\sigma^{\mathrm{G}}}\right]^{-1}\left[\frac{1}{\sigma^{\mathrm{L}}}\int_{D^{\mathrm{L}}(\tau)} dx\,\psi + \frac{1}{\sigma^{\mathrm{G}}}\int_{D^{\mathrm{G}}(\tau)} dx\,\psi\right] \\ &- \left[\frac{X}{\sigma^{\mathrm{L}}} + \frac{1-X}{\sigma^{\mathrm{G}}}\right]^{-1}\left[\frac{1}{\sigma^{\mathrm{L}}}\int_0^X dx\,\psi + \frac{1}{\sigma^{\mathrm{G}}}\int_X^1 dx\,\psi\right]. \end{aligned} \tag{3.28}$$

From the piece-wise linear nature of $\psi(x,t)$, the integrals are calculated by the trapezoidal rule as

$$\int_{D^{\mathrm{L}}} dx\ \psi(x,t) = \frac{1}{2}|D^{\mathrm{L}}|\left(\psi(\hat{X}_\uparrow(t),t) + \psi(\hat{X}_\downarrow(t),t)\right), \tag{3.29}$$

$$\int_{D^{\mathrm{G}}} dx\ \psi(x,t) = \frac{1}{2}|D^{\mathrm{G}}|\left(\psi(\hat{X}_\uparrow(t),t) + \psi(\hat{X}_\downarrow(t),t)\right), \tag{3.30}$$

where $\psi(X_\uparrow(t)+1) = \psi(X_\uparrow(t))$ is applied. Using these relations, we obtain

$$\frac{1}{\sigma^{\mathrm{L}}}\int_{D^{\mathrm{L}}} dx\ \psi + \frac{1}{\sigma^{\mathrm{G}}}\int_{D^{\mathrm{G}}} dx\ \psi = \frac{1}{2}\left(\frac{|D^{\mathrm{L}}|}{\sigma^{\mathrm{L}}} + \frac{|D^{\mathrm{G}}|}{\sigma^{\mathrm{G}}}\right)\left(\psi(\hat{X}_\uparrow(t),t) + \psi(\hat{X}_\downarrow(t),t)\right). \tag{3.31}$$

Substituting this into (3.28), we have

$$q(\tau) = \frac{1}{2}\left(\psi(\hat{X}_\uparrow(\tau),\tau) + \psi(\hat{X}_\downarrow(\tau),\tau)\right) - \frac{1}{2}\left(\psi(0,0) + \psi(X,0)\right). \tag{3.32}$$

Here,

$$\psi(0,0) = 0, \qquad \psi(X,0) = (\rho_X^{\mathrm{L}} - \bar{\rho})X, \tag{3.33}$$

and

$$\psi(\hat{X}_\uparrow(\tau),\tau) = \psi(X_\uparrow(\tau),\tau), \qquad \psi(\hat{X}_\downarrow(\tau),\tau) = \psi(X_\downarrow(\tau),\tau). \tag{3.34}$$

We thus obtain

$$\lim_{\tau\to\infty}\langle q(\tau)\rangle^{\mathrm{eq}}_{\boldsymbol{\rho}_X^{\phi=0}\to *} = \frac{1}{2}\lim_{\tau\to\infty}\left(\langle\psi(X_\uparrow(\tau),\tau)\rangle + \langle\psi(X_\downarrow(\tau),\tau)\rangle\right) - \frac{1}{2}(\rho_X^{\mathrm{L}} - \bar{\rho})X. \tag{3.35}$$

Note that the positions of the interfaces, $X_\uparrow$ and $X_\downarrow$, are uniformly distributed in the interval $x \in [0,1]$ as $\tau \to \infty$. We thus conclude that

$$\langle Q\rangle^{\mathrm{eq}}_{\boldsymbol{\rho}_X^{\phi=0}} = L\left[C - \frac{1}{2}(\rho_X^{\mathrm{L}} - \bar{\rho})X\right], \tag{3.36}$$

where C is a constant independent of X. Using the relation

$$\bar{\rho} = X\rho_X^{\mathrm{L}} + (1-X)\rho_X^{\mathrm{G}}, \tag{3.37}$$

which comes from (2.43), we can also express (3.36) as

$$\langle Q\rangle^{\mathrm{eq}}_{\boldsymbol{\rho}_X^{\phi=0}} = L\left[C - \frac{1}{2}(\rho_X^{\mathrm{L}} - \rho_X^{\mathrm{G}})X(1-X)\right]. \tag{3.38}$$

Substituting (3.38) into (3.5), we have

$$\mathcal{F}_{\mathrm{ss}}(X;\bar{\rho},\phi) = L\left[\int_0^1 dx\ f(\rho_X^\phi(x)) - \frac{\phi}{2}(\rho_X^{\mathrm{L}} - \rho_X^{\mathrm{G}})X(1-X) + \phi C\right]. \tag{3.39}$$

We note that $\rho_X^\phi(x)$ is uniquely determined for given $(X,\phi,\bar{\rho})$ by $\mu(\rho_X^\phi(x)) = \mu_X^\phi(x)$ with (2.39) and (2.40) and that ρ_X^{L} and ρ_X^{G} are functions of $(X,\bar{\rho})$. Thus, $\mathcal{F}_{\mathrm{ss}}(X;\bar{\rho},\phi)$ is the variational function for determining the most probable interface position X_* for a given $(\bar{\rho},\phi)$. The most probable density profile is expressed as $\rho_{X_*}^\phi(x)$.

4 Variational Equation

In this section, using the variational function (3.39), we determine the most probable value of X. This is regarded as an extension of the argument for determining the equilibrium profile in the paragraph containing (2.23). Thus, similarly to (2.23), we analyze the variational equation

$$\left. \frac{d\mathcal{F}_{\mathrm{ss}}(X;\bar{\rho},\phi)}{dX} \right|_{X=X_*} = 0 \tag{4.1}$$

with (3.39). The difference from (2.23) is the $O(\phi)$ terms in (3.39). As shown in Fig. 4, one of the interfaces of $\rho_X^\phi(x)$ is located at $x = 0$ for any X, both the liquid and gas density profiles are sloped, and the chemical potential profile $\mu_X^\phi(x)$ is piece-wise linear. Then, as did for the equilibrium system, we first derive the chemical potential at the interface $\mu_{X_*}^{\mathrm{I}}$ defined by (2.38) instead of directly calculating X_*. Once we have $\mu_{X_*}^{\mathrm{I}}$, we obtain the most probable profiles $\mu_{X_*}^\phi(x)$ and $\rho_{X_*}^\phi(x)$, and the value of X_*. The determination of $\mu_{X_*}^{\mathrm{I}}$ is also physically important because if $\mu_{X_*}^{\mathrm{I}} \neq \mu_{\mathrm{c}}$, metastable states at equilibrium stably appear in the non-equilibrium phase coexistence.

4.1 Preliminaries for the Calculation

In the argument below, we ignore the contribution of $O(\phi^2)$. We first define

$$\bar{\rho}_X^{\mathrm{L}} \equiv \frac{1}{X}\int_0^X dx\,\rho_X^\phi(x), \quad \bar{\rho}_X^{\mathrm{G}} \equiv \frac{1}{1-X}\int_X^1 dx\,\rho_X^\phi(x), \tag{4.2}$$

and

$$\bar{\mu}_X^{\mathrm{L}} \equiv \frac{1}{X}\int_0^X dx\,\mu_X^\phi(x), \quad \bar{\mu}_X^{\mathrm{G}} \equiv \frac{1}{1-X}\int_X^1 dx\,\mu_X^\phi(x). \tag{4.3}$$

Because the density profile $\rho_X^\phi(x)$ and the chemical potential profile $\mu_X^\phi(x)$ are linear in the respective regions, $[0, X]$ and $[X, 1]$, we obtain

$$f\left(\bar{\rho}_X^{\mathrm{L}}\right) = \frac{1}{X}\int_0^X dx f(\rho_X^\phi(x)), \qquad f\left(\bar{\rho}_X^{\mathrm{G}}\right) = \frac{1}{1-X}\int_X^1 dx f(\rho_X^\phi(x)), \tag{4.4}$$

and

$$\bar{\mu}_X^{\mathrm{L}} = \mu(\bar{\rho}_X^{\mathrm{L}}), \qquad \bar{\mu}_X^{\mathrm{G}} = \mu(\bar{\rho}_X^{\mathrm{G}}). \tag{4.5}$$

The pressures in the liquid and gas regions are characterized by $p_X^{\mathrm{L}} \equiv p(\bar{\rho}_X^{\mathrm{L}})$ and $p_X^{\mathrm{G}} \equiv p(\bar{\rho}_X^{\mathrm{G}})$, which are expressed by

$$p_X^{\mathrm{L}} = \mu_X^{\mathrm{L}}\bar{\rho}_X^{\mathrm{L}} - f(\bar{\rho}_X^{\mathrm{L}}), \qquad p_X^{\mathrm{G}} = \mu_X^{\mathrm{G}}\bar{\rho}_X^{\mathrm{G}} - f(\bar{\rho}_X^{\mathrm{G}}). \tag{4.6}$$

The first term on the right side of (3.39) is written as

$$\int_0^1 dx\ f(\rho_X^\phi(x)) = Xf\left(\bar{\rho}_X^{\mathrm{L}}\right) + (1-X)f\left(\bar{\rho}_X^{\mathrm{G}}\right) + O(\phi^2), \tag{4.7}$$

and the variational function (3.5) as

$$\mathcal{F}_{\mathrm{ss}}(X;\bar{\rho},\phi) = L\left[Xf\left(\bar{\rho}_X^{\mathrm{L}}\right) + (1-X)f\left(\bar{\rho}_X^{\mathrm{G}}\right) - \frac{\phi}{2}\left(\rho_X^{\mathrm{L}} - \rho_X^{\mathrm{G}}\right)X(1-X) + \phi C\right]. \tag{4.8}$$

Since $\bar\rho_X^{\rm L}=\rho_X^{\rm L}+O(\phi)$ and $\bar\rho_X^{\rm G}=\rho_X^{\rm G}+O(\phi)$, we can rewrite (4.8) as

$$\mathcal{F}_{\rm ss}(X;\bar\rho,\phi)=L\left[Xf\left(\bar\rho_X^{\rm L}\right)+(1-X)f\left(\bar\rho_X^{\rm G}\right)-\frac{\phi}{2}\left(\bar\rho_X^{\rm L}-\bar\rho_X^{\rm G}\right)X(1-X)+\phi C\right]. \quad (4.9)$$

We emphasize that (4.9) is explicitly expressed as a function of X.

Noting that the chemical potential profile is piece-wise linear as shown in Fig. 4, we estimate

$$\bar\mu_X^{\rm L}=\frac{\mu_X^\phi(0)+\mu_X^{\rm I}}{2},\qquad \bar\mu_X^{\rm G}=\frac{\mu_X^\phi(1)+\mu_X^{\rm I}}{2}. \quad (4.10)$$

From (4.10), $\phi=\mu_X^\phi(1)-\mu_X^\phi(0)$ is rewritten as

$$\bar\mu_X^{\rm L}-\bar\mu_X^{\rm G}=\frac{\phi}{2}. \quad (4.11)$$

Furthermore, using (2.39) and (2.40), we can express $\bar\mu_X^{\rm L}$ and $\bar\mu_X^{\rm G}$ in terms of $\mu_X^{\rm I}$ as

$$\bar\mu_X^{\rm L}=\mu_X^{\rm I}+\frac{JL}{\sigma^{\rm L}}\frac{X}{2},\quad \bar\mu_X^{\rm G}=\mu_X^{\rm I}-\frac{JL}{\sigma^{\rm G}}\frac{1-X}{2}. \quad (4.12)$$

4.2 Steady State

We consider the variational equation

$$\frac{d\mathcal{F}_{\rm ss}(X;\bar\rho,\phi)}{dX}=0. \quad (4.13)$$

Substituting (4.9) into (4.13), we have

$$\begin{aligned}&f(\bar\rho_X^{\rm L})-f(\bar\rho_X^{\rm G})-\frac{\phi}{2}(\bar\rho_X^{\rm L}-\bar\rho_X^{\rm G})(1-2X)\\&+\bar\mu_X^{\rm L}\frac{d\bar\rho_X^{\rm L}}{dX}X+\bar\mu_X^{\rm G}\frac{d\bar\rho_X^{\rm G}}{dX}(1-X)-\frac{\phi}{2}\left(\frac{d\bar\rho_X^{\rm L}}{dX}-\frac{d\bar\rho_X^{\rm G}}{dX}\right)X(1-X)\\&=0. \end{aligned}\quad (4.14)$$

Using (4.11), we rewrite the second line as

$$[X\bar\mu_X^{\rm L}+(1-X)\bar\mu_X^{\rm G}]\left[X\frac{d\bar\rho_X^{\rm L}}{dX}+(1-X)\frac{d\bar\rho_X^{\rm G}}{dX}\right]. \quad (4.15)$$

Here, taking the derivative of $\bar\rho=X\bar\rho_X^{\rm L}+(1-X)\bar\rho_X^{\rm G}$ in X, we obtain

$$X\frac{d\bar\rho_X^{\rm L}}{dX}+(1-X)\frac{d\bar\rho_X^{\rm G}}{dX}=-(\bar\rho_X^{\rm L}-\bar\rho_X^{\rm G}). \quad (4.16)$$

We substitute this into (4.15) and combine it with (4.14). Then, the variational equation (4.14) becomes

$$f(\bar\rho_X^{\rm L})-f(\bar\rho_X^{\rm G})-(\bar\rho_X^{\rm L}-\bar\rho_X^{\rm G})[(1-X)\bar\mu_X^{\rm L}+X\bar\mu_X^{\rm G}]=0. \quad (4.17)$$

The solution of (4.17) provides the most probable value X_* of the interface position. Therefore, we express

$$f(\bar\rho_{X_*}^{\rm L})-f(\bar\rho_{X_*}^{\rm G})-(\bar\rho_{X_*}^{\rm L}-\bar\rho_{X_*}^{\rm G})[(1-X_*)\bar\mu_{X_*}^{\rm L}+X\bar\mu_{X_*}^{\rm G}]=0. \quad (4.18)$$

Now, we rewrite (4.18) as a different form using the chemical potential at the interface position X_*. We subtract the equilibrium version of (4.18), i.e., $f(\rho_{\mathrm{c}}^{\mathrm{L}}) - f(\rho_{\mathrm{c}}^{\mathrm{G}}) - (\rho_{\mathrm{c}}^{\mathrm{L}} - \rho_{\mathrm{c}}^{\mathrm{G}})\mu_{\mathrm{c}} = 0$, from (4.18). Noting $f(\bar{\rho}_{X_*}^{\mathrm{L}}) - f(\rho_{\mathrm{c}}^{\mathrm{L}}) = (\bar{\rho}_{X_*}^{\mathrm{L}} - \rho_{\mathrm{c}}^{\mathrm{L}})\mu_{\mathrm{c}} + O(\phi^2)$, we obtain

$$(\bar{\rho}_{X_*}^{\mathrm{L}} - \bar{\rho}_{X_*}^{\mathrm{G}})\left\{\mu_{\mathrm{c}} - [(1 - X_*)\bar{\mu}_{X_*}^{\mathrm{L}} + X_*\bar{\mu}_{X_*}^{\mathrm{G}}]\right\} = 0. \tag{4.19}$$

Substituting (4.12) into this equation and using $\bar{\rho}_{X_*}^{\mathrm{L}} \neq \bar{\rho}_{X_*}^{\mathrm{G}}$, we have

$$\mu_{X_*}^{\mathrm{I}} = \mu_{\mathrm{c}} - \frac{JLX_*(1 - X_*)}{2}\left(\frac{1}{\sigma^{\mathrm{L}}} - \frac{1}{\sigma^{\mathrm{G}}}\right). \tag{4.20}$$

Because $X_* = X^{\mathrm{eq}} + O(\phi)$, we can rewrite it as

$$\mu_{X_*}^{\mathrm{I}} = \mu_{\mathrm{c}} - \frac{JLX^{\mathrm{eq}}(1 - X^{\mathrm{eq}})}{2}\left(\frac{1}{\sigma^{\mathrm{L}}} - \frac{1}{\sigma^{\mathrm{G}}}\right). \tag{4.21}$$

Furthermore, combining (2.42) with (4.21), we finally obtain

$$\mu_{X_*}^{\mathrm{I}} = \mu_{\mathrm{c}} + \frac{\phi}{2}\frac{(\sigma^{\mathrm{L}} - \sigma^{\mathrm{G}})X^{\mathrm{eq}}(1 - X^{\mathrm{eq}})}{\sigma^{\mathrm{G}}X^{\mathrm{eq}} + \sigma^{\mathrm{L}}(1 - X^{\mathrm{eq}})}. \tag{4.22}$$

Recalling that X^{eq} is uniquely determined by $\bar{\rho}$ from (2.18), we conclude that $\mu_{X_*}^{\mathrm{I}}$ is expressed in terms of the system parameters. Thus, the chemical potential at the interface deviates from μ_{c} linearly with the voltage ϕ. This means that metastable states at equilibrium stably appear around the interface. The relation (4.22) is the most important achievement of our theory.

Next, from (4.11) and (4.19), we obtain

$$\bar{\mu}_{X_*}^{\mathrm{L}} = \mu_{\mathrm{c}} + X^{\mathrm{eq}}\frac{\phi}{2}, \quad \bar{\mu}_{X_*}^{\mathrm{G}} = \mu_{\mathrm{c}} - (1 - X^{\mathrm{eq}})\frac{\phi}{2}, \tag{4.23}$$

which also gives $\mu_{X_*}^{\phi}(0)$ and $\mu_{X_*}^{\phi}(1)$ using (4.10). The result yields $\mu_{X_*}^{\phi}(x)$. Using $\mu_{X_*}^{\phi}(x) = \mu(\rho_{X_*}^{\phi}(x))$, we have $\rho_{X_*}^{\phi}(x)$. Finally, from $X_*\bar{\rho}_{X_*}^{\mathrm{L}} + (1 - X_*)\bar{\rho}_{X_*}^{\mathrm{G}} = \bar{\rho}$, we can express $X_* - X^{\mathrm{eq}}$ in terms of system parameters. In this manner, all thermodynamic quantities are determined by the variational principle. As one example, we discuss the pressure in the steady state. Using (4.6), we can express (4.18) as

$$p_{X_*}^{\mathrm{L}} - p_{X_*}^{\mathrm{G}} = \frac{\phi\bar{\rho}}{2}. \tag{4.24}$$

Recalling that the local pressure is given by $p(x) = p(\rho(x))$, we define the pressures at the left and right sides of the interface as

$$p_- \equiv \lim_{x \to X_*^-} p(\rho(x)), \qquad p_+ \equiv \lim_{x \to X_*^+} p(\rho(x)). \tag{4.25}$$

Then, using

$$\rho_{X_*}^{\mathrm{L/G}}(\mu_{X_*}^{\mathrm{L/G}} - \mu_{X_*}^{\mathrm{I}}) = p_{X_*}^{\mathrm{L/G}} - p_{-/+}, \tag{4.26}$$

we can derive

$$p_- = p_{\mathrm{c}} + (\mu_{X_*}^{\mathrm{I}} - \mu_{\mathrm{c}})\rho_{\mathrm{c}}^{\mathrm{L}}, \qquad p_+ = p_{\mathrm{c}} + (\mu_{X_*}^{\mathrm{I}} - \mu_{\mathrm{c}})\rho_{\mathrm{c}}^{\mathrm{G}}, \tag{4.27}$$

where p_{c} is the equilibrium coexistence pressure. This result indicates that the pressure is not continuous at the interface. It should be noted that this discontinuity occurs only in the singular continuum description for $\kappa_\Lambda \ll 1$ but never occur in the continuum description for $\kappa_\Lambda \gg 1$ as shown in Appendix B.

5 Global Thermodynamics

The extension of the variational function from $\mathcal{F}_{\rm eq}(X;\bar{\rho})$ to $\mathcal{F}_{\rm ss}(X;\bar{\rho},\phi)$ is closely related to the extension of thermodynamic functions. Without analyzing specific stochastic models, one can construct such an extended thermodynamic framework relying on the consistency, uniqueness, and predictability. This phenomenological argument, which is called *global thermodynamics*, was developed for heat conduction systems exhibiting phase coexistence [9–11]. Furthermore, global thermodynamics was applied to the order–disorder transition in heat conduction, and the prediction by global thermodynamics was confirmed by numerical simulations [12]. Similarly, in the present setup, we can determine the variational function (4.9) following the method in Refs. [11, 28].

We set $M \equiv \bar{\rho}L$, where MA represents the total number of particles in the tube. In equilibrium thermodynamics, the free energy function $F_{\rm eq}(L,M)$ is determined as

$$F_{\rm eq}(L,M)=\mathcal{F}_{\rm eq}(X_*;\bar{\rho}) \tag{5.1}$$

using the variational function $\mathcal{F}_{\rm eq}(X;\bar{\rho})$ given by (2.21). We then have the fundamental relation of thermodynamics

$$dF_{\rm eq}=-p_{\rm c}dL+\mu_{\rm c}dM, \tag{5.2}$$

where $p_{\rm c}$ and $\mu_{\rm c}$ are the equilibrium values of pressure and chemical potential in phase coexistence states. Note that $p_{\rm c}$ and $\mu_{\rm c}$ are constants in (L,M). Extending the relations (5.1) and (5.2) to non-equilibrium systems, we attempt to determine the thermodynamic function $F_{\rm ss}(L,M,\phi)$ and the variational function $\mathcal{F}_{\rm ss}(X;\bar{\rho},\phi)$.

5.1 Thermodynamic Function

For the system under consideration, we have the equilibrium free energy $F_{\rm eq}(L,M)$. In the phase coexistence state, it takes the simple form

$$F_{\rm eq}(L,M)=-p_{\rm c}L+\mu_{\rm c}M. \tag{5.3}$$

To derive $F_{\rm ss}(L,M,\phi)$, we first assume

$$dF_{\rm ss}=-\bar{p}dL+\bar{\mu}dM-\Psi d\phi. \tag{5.4}$$

without an explicit form of Ψ, where $\bar{p}$ and $\bar{\mu}$ are the average pressure and chemical potential defined by

$$\bar{p}=X_*p^{\rm L}_{X_*}+(1-X_*)p^{\rm G}_{X_*},\qquad \bar{\mu}=X_*\bar{\mu}^{\rm L}_{X_*}+(1-X_*)\bar{\mu}^{\rm G}_{X_*}. \tag{5.5}$$

Note that $\bar{p}$ and $\bar{\mu}$ are functions of $(\bar{\rho},\phi)$ and that the steady state value X_* of the interface position is also given as a function of $(\bar{\rho},\phi)$. Ψ is a conjugate variable of the battery voltage ϕ. From the reflection symmetry, Ψ is an odd function of ϕ and thus $\Psi=0$ for $\phi=0$. On the other hand, from the singular nature of the phase coexistence, we assume that $\Psi\neq 0$ in the limit $\phi\to 0+$. For simplicity, we consider only the case $\phi>0$ as in the previous sections and we can set $\Psi=\Psi(L,M)$ by considering the limit $\phi\to 0+$ to study the linear response regime. Furthermore, from the extensivity in the equilibrium state, we have

$$\Psi(L,M)=M\psi(v) \tag{5.6}$$

with $v=L/M=1/\bar{\rho}$.

Next, we set

$$F_{\rm ss}(L,M,\phi)=F_{\rm eq}(L,M)-M\psi(v)\phi \tag{5.7}$$

in the linear response regime. By substituting this expression into (5.4), we obtain

$$\bar{p}=p_{\rm c}+\psi'(v)\phi, \qquad \bar{\mu}=\mu_{\rm c}+(v\psi'(v)-\psi(v))\phi. \tag{5.8}$$

We solve these differential equations of $\psi(v)$. Eliminating $\psi'(v)$ from these two equations, we obtain a necessary condition for $\psi(v)$ as

$$\psi(v)\phi=v(\bar{p}-p_{\rm c})-(\bar{\mu}-\mu_{\rm c}). \tag{5.9}$$

Here, we simplify the right-hand side of (5.9) using the expressions given in (5.5). We first note the relations

$$p^{\rm L}_{X_*}-p_{\rm c}=\bar{\rho}^{\rm L}_{X_*}(\bar{\mu}^{\rm L}_{X_*}-\mu_{\rm c}), \qquad p^{\rm G}_{X_*}-p_{\rm c}=\bar{\rho}^{\rm G}_{X_*}(\bar{\mu}^{\rm G}_{X_*}-\mu_{\rm c}). \tag{5.10}$$

Using the relations, we express (5.9) as

$$\psi(v)\phi=(v\bar{\rho}^{\rm L}_{X_*}-1)X_*\bar{\mu}^{\rm L}_{X_*}+(v\bar{\rho}^{\rm G}_{X_*}-1)(1-X_*)\bar{\mu}^{\rm G}_{X_*}. \tag{5.11}$$

We next notice that the relation (3.37) yields useful expressions

$$(v\bar{\rho}^{\rm L}_{X_*}-1)X_*+(v\bar{\rho}^{\rm G}_{X_*}-1)(1-X_*)\bar{\mu}^{\rm G}_{X_*}=0, \tag{5.12}$$

and

$$\bar{\rho}^{\rm L}_{X_*}-\bar{\rho}=(1-X_*)(\bar{\rho}^{\rm L}_{X_*}-\bar{\rho}^{\rm G}_{X_*}). \tag{5.13}$$

Using (4.11) and (5.12), we rewrite (5.11) as

$$\psi(v)\phi=(v\bar{\rho}^{\rm L}_{X_*}-1)X_*\frac{\phi}{2}. \tag{5.14}$$

By substituting (5.13) into (5.14), we obtain

$$\phi\Psi(L,M)=\phi M\psi(v)=\frac{\phi}{2}L(\bar{\rho}^{\rm L}_{X_*}-\bar{\rho}^{\rm G}_{X_*})X_*(1-X_*). \tag{5.15}$$

Thus, if a solution exists for (5.8), this should be (5.15).

Conversely, suppose that (5.15) holds. Noting the relation

$$F_{\rm eq}(L,M)=LX_*f(\bar{\rho}^{\rm L}_{X_*})+L(1-X_*)f(\bar{\rho}^{\rm G}_{X_*})+O(\phi^2), \tag{5.16}$$

we find that $F_{\rm ss}$ assumed in (5.7) is expressed as

$$F_{\rm ss}(L,M,\phi)=LX_*f(\bar{\rho}^{\rm L}_{X_*})+L(1-X_*)f(\bar{\rho}^{\rm G}_{X_*})-\frac{\phi}{2}L(\bar{\rho}^{\rm L}_{X_*}-\bar{\rho}^{\rm G}_{X_*})X_*(1-X_*). \tag{5.17}$$

Then, using (4.6) and (4.11), we rewrite (5.17) as

$$F_{\rm ss}(L,M,\phi)=-LX_*p^{\rm L}_{X_*}-L(1-X_*)p^{\rm G}_{X_*}+(X_*\bar{\mu}^{\rm L}_{X_*}+(1-X)\bar{\mu}^{\rm G}_{X_*})M. \tag{5.18}$$

Furthermore, using (5.5), we further rewrite $F_{\rm ss}$ as a suggestive form

$$F_{\rm ss}(L,M,\phi)=-\bar{p}L+\bar{\mu}M. \tag{5.19}$$

Now, taking the derivative of $F_{\rm ss}$ in L, we have

$$\frac{\partial F_{\rm ss}(L,M,\phi)}{\partial L}=-\bar{p}-\frac{\partial \bar{p}(L,M,\phi)}{\partial L}L+\frac{\partial \bar{\mu}(L,M,\phi)}{\partial L}M. \tag{5.20}$$

Here, using (4.5), (4.6), (4.11), and (4.24), we can confirm

$$\frac{\partial \bar{p}(L,M,\phi)}{\partial L}=\bar{\rho}\frac{\partial \bar{\mu}(L,M,\phi)}{\partial L}. \tag{5.21}$$

Substituting this result into (5.20), we obtain

$$\frac{\partial F_{\rm ss}(L,M,\phi)}{\partial L}=-\bar{p}. \tag{5.22}$$

By repeating the similar calculation, we also have

$$\frac{\partial F_{\rm ss}(L,M,\phi)}{\partial M}=\bar{\mu}. \tag{5.23}$$

Finally, (5.15) leads to

$$\Psi=-\frac{\partial F_{\rm ss}(L,M,\phi)}{\partial \phi}. \tag{5.24}$$

These three relations (5.22), (5.23), and (5.24) are summarized as an extended form of the fundamental relation of thermodynamics (5.4). This means that $\psi(v)$ given by (5.15) satisfies (5.8). We then conclude that (5.17) is the free energy extended to the non-equilibrium steady state.

5.2 Variational Function

We formulate a variational principle for determining the steady state. In the phase coexistence state, unconstrained thermodynamic variables are the length of the liquid region LX and the particle number of the liquid $M^{\rm L}\equiv L\rho^{L}$ per unit area. Let $\mathcal{F}_{\rm ss}(LX,M^{\rm L};L,M,\phi)$ be the variational function for $(LX,M^{\rm L})$ with (L,M,ϕ) fixed. Following the standard method of thermodynamics, we assume

$$F_{\rm ss}(L,M,\phi)=\min_{X,M^{\rm L}}\mathcal{F}_{\rm ss}(LX,M^{\rm L};L,M,\phi). \tag{5.25}$$

With (5.17), (5.25) naturally leads to

$$\mathcal{F}_{\rm ss}(LX,M^{\rm L};L,M,\phi)=F_{\rm eq}(LX,M^{\rm L})+F_{\rm eq}(L(1-X),M^{\rm L})-\frac{\phi}{2}(M^{\rm L}-MX), \tag{5.26}$$

where we have used (5.14). The variational equations are then expressed as

$$\frac{\partial \mathcal{F}_{\rm ss}(LX,M^{\rm L};L,M,\phi)}{\partial X}=0, \tag{5.27}$$

and

$$\frac{\partial \mathcal{F}_{\rm ss}(LX,M^{\rm L};L,M,\phi)}{\partial M^{\rm L}}=0. \tag{5.28}$$

The solution $(X_*,M^{\rm L}_*)$ of the equations is the steady state value.

Now, we construct a variational function for determining X_* from the variational function (5.26) for determining X_* and M_*^{L}. For a given X, we write the solution of (5.28) as M_X^{L}. We can then confirm

$$\left.\frac{d\mathcal{F}_{\mathrm{ss}}(LX, M_X^{\mathrm{L}}; L, M, \phi)}{dX}\right|_{X=X_*} = 0 \tag{5.29}$$

using (5.27) and (5.28). The Eq. (5.29) means that $\mathcal{F}_{\mathrm{ss}}(LX, M_X^{\mathrm{L}}; L, M, \phi)$ is the variational function for determining X_*. We note that $M_X^{\mathrm{L}} = L\bar{\rho}_X^{\mathrm{L}}$ because (5.28) leads to (4.11). Thus, the variational function $\mathcal{F}_{\mathrm{ss}}(LX, M_X^{\mathrm{L}}; L, M, \phi)$ takes the same form as (3.39) expect for the constant term. Namely, the steady state determined by the phenomenological argument is equivalent to that calculated in the previous section. Therefore, all the prediction made by global thermodynamics for the present setup are the same as the theoretical result for the stochastic model we study. In our research history, the variational function (4.9) was first derived using global thermodynamics, and after that it was re-derived by analyzing the stochastic model.

6 Numerical Simulation

In this section, we perform numerical simulations of the discrete model and compare numerical results with the theoretical predictions presented in the previous sections. More explicitly, the time evolution of $(\rho_i)_{i=1}^N$ is defined by (2.8) accompanied with the current $(j_i)_{i=1}^N$ defined by (2.10). To obtain $(j_i)_{i=1}^N$ using (2.10), we determine $(\tilde{\mu}_i)_{i=1}^N$ by (2.9) with

$$\mu(\rho_i) = (\rho_i - 0.5)(\rho_i - 1.5)(\rho_i - 2.5) \tag{6.1}$$

from (2.6). We adopt a simple form of the conductivity $\sigma(\rho) = \rho$, where we have introduced a dimensionless time in this expression. For this specific model, we have $\rho_{\mathrm{c}}^{\mathrm{L}} = 2.5$, $\rho_{\mathrm{c}}^{\mathrm{G}} = 0.5$, and $\mu_{\mathrm{c}} = 0$ from (2.16), and we thus obtain $\sigma^{\mathrm{L}} = 2.5$ and $\sigma^{\mathrm{G}} = 0.5$ from (2.29).

Recalling that the independent parameters to be specified for numerical determination of the steady state are $(\kappa_\Lambda, T_{\mathrm{eff}}, \phi, \bar{\rho}, N)$ as discussed around (2.13), we study the κ_Λ dependence of the steady state with fixing the other parameter values as

$$(T_{\mathrm{eff}}, \phi, \bar{\rho}, N) = (0.002, 0.05, 1.5, 64). \tag{6.2}$$

Since A and Λ are contained in the renormalized quantities κ_Λ and T_{eff}, we do not need to specify the values of A and Λ, while the total volume and the total number of particles are given by LA and $\bar{\rho}LA$ with $L = \Lambda N$. To numerically solve (2.8) and (2.10), we adopt the Heun method with a time step $dt = 0.01\Lambda^2$, where it should be noted that the time step dt is always coupled with Λ^2 for the time-discretized form of (2.8) and (2.10).

In Fig. 7, we show the steady state for $\kappa_\Lambda = 0.5$ and $\kappa_\Lambda = 1.5$, where the density profile ρ_i and the chemical potential profile $\tilde{\mu}_i$ are plotted for i/N. We remark that the system reaches the steady state without dependence on initial conditions, $(\rho_i)_{i=1}^N$ at $t = 0$. Note that $\tilde{\mu}_i = \mu_{\mathrm{c}} = 0$ for all i for the equilibrium system with $\phi = 0$, which is shown as the dotted line in Fig. 7b. It is observed that $\tilde{\mu}$ near the interface is close to $\mu_{\mathrm{c}} = 0$ for the case $\kappa_\Lambda = 1.5$, while it clearly deviates from $\mu_{\mathrm{c}} = 0$ for the case $\kappa_\Lambda = 0.5$. That is, the metastable gas stably appears at the left-side of the interface for the case $\kappa_\Lambda = 0.5$.

Here, we determine the chemical potential at the interface, which is denoted by μ^I, more quantitatively from the numerical data $(\rho_i)_{i=1}^N$ and $(\tilde{\mu}_i)_{i=1}^N$. In principle, we first determine the interface position X^I from the data $(\rho_i)_{i=1}^N$, and then read the value of the chemical potential

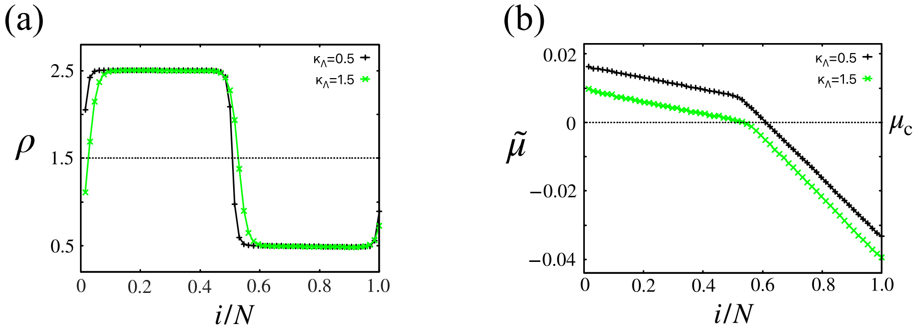

Fig. 7 **a** Density profile ρ_i for i/N. **b** Chemical potential profile $\tilde{\mu}_i$ for i/N. $\kappa_\Lambda = 0.5$ and $\kappa_\Lambda = 1.5$. The dotted line in (**b**) represents the equilibrium profile of chemical potential $\tilde{\mu}_i = \mu_c = 0$

at the interface position from the data $(\tilde{\mu}_i)_{i=1}^N$. In practice, we use the linear interpolation of the data sets to systematically estimate μ^I for several parameters. That is, we define a piecewise linear function $\rho(x)$ for $0 \le x \le 1$ by connecting two consecutive points $(i/N, \rho_i)$ and $((i+1)/N, \rho_{i+1})$ for $0 \le i \le N$ in the graph of $(i/N, \rho_i)_{i=1}^N$. We then define the interface position X^I as $\rho(X^I) = 1.5$, where $(\rho_c^G + \rho_c^L)/2 = 1.5$. Similarly, we define $\tilde{\mu}(x)$ from $(\tilde{\mu}_i)_{i=1}^N$. Using this X^I and $\mu(x)$, we obtain $\mu^I = \tilde{\mu}(X^I)$. More explicitly, μ^I is determined as follows. First, we find i_* satisfying $\rho_{i_*-1} > 1.5$ and $\rho_{i_*} < 1.5$. From the construction of $\rho(x)$, we obtain

$$X^I = \frac{1.5 - \rho_{i_*}}{\rho_{i_*-1} - \rho_{i_*}} \frac{i_* - 1}{N} + \frac{\rho_{i_*-1} - 1.5}{\rho_{i_*-1} - \rho_{i_*}} \frac{i_*}{N}. \tag{6.3}$$

We then have

$$\mu^I = \frac{1.5 - \rho_{i_*}}{\rho_{i_*-1} - \rho_{i_*}} \tilde{\mu}_{i_*-1} + \frac{\rho_{i_*-1} - 1.5}{\rho_{i_*-1} - \rho_{i_*}} \tilde{\mu}_{i_*}. \tag{6.4}$$

Using this formula, we have $\mu^I = 7.7 \times 10^{-3}$ for the data of $\kappa_\Lambda = 0.5$, and $\mu^I = 2.1 \times 10^{-4}$ for the data of $\kappa_\Lambda = 1.5$. In Fig. 8, μ^I obtained by (6.4) are plotted for several values of κ_Λ.

Now, we compare the numerical results with the theoretical predictions. We developed the theory of the steady state in the weak noise limit $T_{\text{eff}} \ll 1$ and the macroscopic limit $N \gg 1$, with particularly focusing on the two regimes $\kappa_\Lambda \gg 1$ and $\kappa_\Lambda \ll 1$. When $\kappa_\Lambda \gg 1$, the chemical potential at the interface is $\mu_c = 0$, as shown in Appendix B. When $\kappa_\Lambda \ll 1$, we have the formula (4.22), where $\mu_c = 0$, $\sigma^L = 2.5$, and $\sigma^G = 1.5$ were already determined for the model in the first paragraph of this section. X^{eq} in the right-side of (4.22) is determined as $X^{eq} = 1/2$ using (2.18) with $\bar{\rho} = 1.5$, $\rho_c^L = 2.5$, $\rho_c^G = 0.5$. By substituting these values into (4.22), we obtain

$$\mu^{\mathrm{I}}_{X_*} = \frac{\phi}{6} + O(\phi^2). \tag{6.5}$$

The dotted lines in Fig. 8 represent the theoretical predictions $\mu^{\mathrm{I}}/\phi = 1/6$ for $\kappa_\Lambda \ll 1$ and $\mu^{\mathrm{I}}/\phi = 0$ for $\kappa_\Lambda \gg 1$. These are consistent with the numerical result in Fig. 8.

It is quite interesting to elucidate the κ_Λ dependence of μ^I quantitatively. In particular, one may conjecture a phase transition at some value of κ_Λ in the limit $N \to \infty$. To investigate the validity of this naive conjecture, we have to numerically study the asymptotic behavior for $N \to \infty$, $T_{\text{eff}} \to 0$ and $\phi \to 0$ in more detail. From the theoretical viewpoint, we need to develop a calculation method for thermodynamic properties of the system with finite κ_Λ.

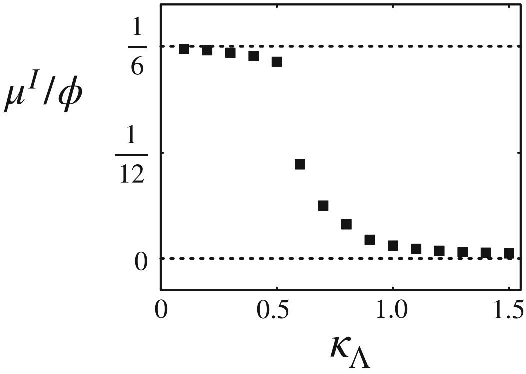

Fig. 8 κ_Λ dependence of μ^I. Square symbols show the numerical results for $N = 64$. The two dotted lines represent the theoretical predictions $\mu^I = \phi/6$ for $\kappa_\Lambda \ll 1$ and $\mu^I = 0$ for $\kappa_\Lambda \gg 1$

7 Concluding Remarks

We have derived the variational function determining the steady state for a boundary-driven diffusive system with $\kappa_\Lambda \ll 1$. The result is consistent with global thermodynamics, which is an extended framework of thermodynamics. Before ending the paper, we present a few remarks.

The first remark is on the boundary conditions. It is natural to study a system with different boundary conditions leading to the same most probable profile. As more familiar boundary conditions, one considers the case that chemical potentials at boundaries are fixed. However, as far as we attempted, we could not evaluate the Zubarev-McLennan representation for this case. To study the boundary condition dependence of the system is a future problem.

Second, in general, fluctuating hydrodynamics is regarded as a mesoscopic model obtained by coarse-graining microscopic dynamics. Thus, it is a significant problem to find relationship between microscopic dynamics and the discrete fluctuating dynamics. As the first step of such studies, parameter values of the model should be determined from the observation of microscopic dynamics. In particular, it seems highly challenging to identify the value of κ_Λ from microscopic models.

Third, as a generalization of the present model, one may consider a discrete fluctuating hydrodynamics describing liquid–gas phase coexistence in heat conduction systems. One can numerically study the model by changing κ_Λ. It is interesting to observe the deviation of the interface temperature from the equilibrium coexistence temperature. Furthermore, following the theoretical method presented in this paper, we may develop a theory for calculating the deviation. We conjecture that the deviation formula is equivalent to that predicted by global thermodynamics.

The most important future work is an experimental observation of non-equilibrium phase coexistence in which metastable states are stable as the influence of a non-equilibrium current. As shown in this paper, the phenomenon is expected to occur in systems described by a discrete fluctuating hydrodynamics. However, it is not obvious whether experimental systems are described by a discrete fluctuating hydrodynamics. It would be interesting to clarify an experimental condition for realizing a discrete fluctuating hydrodynamics.

Appendix A: Derivation of (2.14)

In this section, we derive the the stationary distribution of $\boldsymbol{\rho}$ for the equilibrium system with $\phi = 0$. In general, to analyze statistical properties of $\boldsymbol{\rho}(t)$ obeying (2.8) with (2.10), it is convenient to use a new variable $\boldsymbol{\psi} = (\psi_i)_{i=1}^N$ for $\boldsymbol{\rho}$. The introduction of the new variable is another purpose of this section. See Appendix C for the analysis using $\boldsymbol{\psi}$.

We first define $\psi_i(t)$ by

$$\frac{d\psi_i(t)}{dt} = -j_i(t) \tag{A.1}$$

with $\psi_i(0) = \Lambda \sum_{j=1}^{i} (\rho_j(0) - \bar{\rho})$ at $t = 0$. Substituting (A.1) into (2.8) and integrating it in time, we have

$$\rho_i(t) = \frac{\psi_i(t) - \psi_{i-1}(t)}{\Lambda} + \bar{\rho} \tag{A.2}$$

for any t. Substituting (A.2) into $\mathcal{F}(\boldsymbol{\rho})$ given by (2.7), we can define $\mathcal{F}(\boldsymbol{\psi})$ from $\mathcal{F}(\boldsymbol{\rho})$. Taking the derivative of $\mathcal{F}(\boldsymbol{\psi})$ in ψ_i, we obtain

$$\frac{\partial \mathcal{F}}{\partial \psi_i} = \left(\frac{\partial \mathcal{F}}{\partial \rho_i} - \frac{\partial \mathcal{F}}{\partial \rho_{i+1}} \right) \frac{1}{\Lambda} = \tilde{\mu}_i - \tilde{\mu}_{i+1}. \tag{A.3}$$

Using (A.1) and (A.3), we rewrite (2.10) as

$$\frac{d\psi_i}{dt} = \frac{\sigma(\rho_i^{\mathrm{m}})}{\Lambda} \left(-\frac{\partial \mathcal{F}}{\partial \psi_i} - \phi \delta_{i,N} \right) + \sqrt{\frac{2\sigma(\rho_i^{\mathrm{m}}) T_{\mathrm{eff}}}{\Lambda}} \cdot \xi_i \tag{A.4}$$

with

$$\rho_i^{\mathrm{m}} = \frac{\psi_{i+1} - \psi_{i-1}}{2\Lambda} + \bar{\rho}. \tag{A.5}$$

Because $\sigma(\rho_i^{\mathrm{m}})$ is independent of ψ_i, the multiplication of $\sigma(\rho_i^{\mathrm{m}})$ and ξ_i is uniquely determined independently of the multiplication rule. From (A.4), we obtain the stationary distribution of $\boldsymbol{\psi}$ for the equilibrium system with $\phi = 0$ as

$$\mathcal{P}_{\mathrm{eq}}(\boldsymbol{\psi}) = \frac{1}{Z'} \exp\left[-\frac{1}{T_{\mathrm{eff}}} \mathcal{F}(\boldsymbol{\psi}) \right], \tag{A.6}$$

where Z' is the normalization constant. This gives the stationary distribution of $\boldsymbol{\rho}$ as (2.14).

Appendix B: Analysis of the Continuum Model

In this section, we analyze the continuum model (2.2) and (2.3) which corresponds to the discrete model (2.8) and (2.10) in the limit $\kappa_\Lambda \to \infty$ and $N \to \infty$ with L and κ fixed. Explicitly, we derive the phase coexistence condition (2.16) for the equilibrium system with $\phi = 0$ and the chemical potential at the interface for the case $\phi > 0$.

B.1: Equilibrium Phase Coexistence

Stationary solutions of (2.2) and (2.3) with $\phi = 0$ and $T = 0$ satisfy

$$\partial_x \frac{\delta \mathcal{F}}{\delta \rho(x)} = 0. \tag{B.1}$$

Using (2.5), (B.1) is explicitly written as

$$f'(\rho) - \kappa \partial_x^2 \rho = \mu_{\mathrm{c}}, \tag{B.2}$$

where μ_{c} is a constant in x. Furthermore, multiplying $(\partial_x \rho)$ with (B.2) and integrating in x, we obtain

$$f(\rho) - \frac{\kappa}{2}(\partial_x \rho)^2 - \mu_{\mathrm{c}}\rho = p_{\mathrm{c}}, \tag{B.3}$$

where p_{c} is also a constant in x.

We first consider necessary conditions under which there is a stationary and spatially inhomogeneous solution, which we call the phase coexistence solution, because it connects two stationary and spatially homogeneous solutions that represent a liquid phase and a gas phase, respectively. To make the argument clear, we take the limit $L \to \infty$ and we assume $\rho(0) > \rho(\infty)$ for the phase coexistence solution. Because the phase coexistence solution approaches to the stationary and spatially homogeneous solutions $\rho(0)$ and $\rho(\infty)$ as $x \to 0$ and $x \to \infty$, we have

$$\partial_x \rho(0) = 0, \qquad \partial_x^2 \rho(0) = 0, \qquad \partial_x \rho(\infty) = 0, \qquad \partial_x^2 \rho(\infty) = 0. \tag{B.4}$$

Therefore, (B.2) and (B.3) lead to necessary conditions as

$$\mu(\rho(0)) = \mu(\rho(\infty)) = \mu_{\mathrm{c}}, \tag{B.5}$$

and

$$f(\rho(0)) - \mu_{\mathrm{c}}\rho(0) = f(\rho(\infty)) - \mu_{\mathrm{c}}\rho(\infty) = p_{\mathrm{c}}, \tag{B.6}$$

which is further rewritten as

$$\mu_{\mathrm{c}} = \frac{f(\rho(0)) - f(\rho(\infty))}{\rho(0) - \rho(\infty)}. \tag{B.7}$$

For the function $f(\rho)$ with two local minima, the conditions (B.5) and (B.7) represents the common tangent line at the special values $\rho = \rho_{\mathrm{c}}^{\mathrm{L}}$ and $\rho = \rho_{\mathrm{c}}^{\mathrm{G}}$. We set $\rho_{\mathrm{c}}^{\mathrm{L}} > \rho_{\mathrm{c}}^{\mathrm{G}}$ without loss of generality. We thus identify $\rho(0) = \rho_{\mathrm{c}}^{\mathrm{L}}$ and $\rho(\infty) = \rho_{\mathrm{c}}^{\mathrm{G}}$, and the values of the constants μ_{c} and p_{c} are also determined. Note that (B.5) and (B.6) are regarded as the conditions giving $\rho_{\mathrm{c}}^{\mathrm{L}}$, $\rho_{\mathrm{c}}^{\mathrm{G}}$, μ_{c} and p_{c} by the form

$$\mu(\rho_{\mathrm{c}}^{\mathrm{L}}) = \mu(\rho_{\mathrm{c}}^{\mathrm{G}}) = \mu_{\mathrm{c}}, \qquad p(\rho_{\mathrm{c}}^{\mathrm{L}}) = p(\rho_{\mathrm{c}}^{\mathrm{G}}) = p_{\mathrm{c}}. \tag{B.8}$$

Now, suppose that $\bar{\rho}$ satisfies $\rho_{\mathrm{c}}^{\mathrm{G}} < \bar{\rho} < \rho_{\mathrm{c}}^{\mathrm{L}}$, where $\rho_{\mathrm{c}}^{\mathrm{G}}$ and $\rho_{\mathrm{c}}^{\mathrm{L}}$ are determined by (B.8). By setting $\rho(0) = \rho_{\mathrm{c}}^{\mathrm{L}}$ and $\rho(\infty) = \rho_{\mathrm{c}}^{\mathrm{G}}$, we solve (B.2) with the determined value of μ_{c}. We here notice that (B.2) is interpreted as Newton's equation describing the motion of a point particle under a potential field, where ρ and x correspond to position and time, respectively. κ is interpreted as the mass, and the potential function $V(\rho)$ is given by $V(\rho) \equiv \mu_{\mathrm{c}}\rho - f(\rho)$. (B.3) represents the energy conservation for the equation of motion. From (B.8), we find that $\rho_{\mathrm{c}}^{\mathrm{L}}$ and $\rho_{\mathrm{c}}^{\mathrm{G}}$ are local maximal points with the same potential value. Therefore, the phase coexistence solution $\rho(x)$ with $\rho(0) = \rho_{\mathrm{c}}^{\mathrm{L}}$ and $\rho(\infty) = \rho_{\mathrm{c}}^{\mathrm{G}}$ is given by the heteroclinic orbit connecting the two maximal points with the same potential value. This result corresponds to the statement involving (2.16) in the main text.

B.2: Non-equilibrium Phase Coexistence

Stationary solutions of (2.2) and (2.3) with $\phi > 0$ and $T = 0$ satisfy

$$\partial_x \frac{\delta \mathcal{F}}{\delta \rho(x)} = -\frac{J}{\sigma(\rho(x))}, \tag{B.9}$$

which corresponds to (2.27) in the continuum limit $\kappa_\Lambda \to \infty$ and $N \to \infty$, where J is a constant given by

$$J = \left(\int_0^L dx \, \frac{1}{\sigma(\rho(x))} \right)^{-1}, \tag{B.10}$$

which corresponds to (2.28) in the continuum limit $\kappa_\Lambda \to \infty$ and $N \to \infty$. By analyzing (B.9), we determine the value of the chemical potential at the interface.

First, to uniquely identify the interface position, we introduce a scaled coordinate $\hat{x} = x/L$. Taking the limit $L \to \infty$, we find that the interface width in the scaled coordinate space becomes zero. Thus, the interface position X in the $\hat{x}$ space is given by the discontinuous point of $\rho(\hat{x})$ in the limit $L \to \infty$. We then define the chemical potential at the interface by $\mu(\hat{x} = X)$. To determine the value of $\mu(\hat{x} = X)$, we consider the generalized chemical potential $\tilde{\mu}(x)$ given by

$$\tilde{\mu}(x) = \mu(\rho(x)) - \kappa \partial_x^2 \rho, \tag{B.11}$$

which corresponds to (2.12) in the limit $\kappa_\Lambda \to \infty$ and $N \to \infty$. By integrating (B.9) in the range $[x_1, x_2]$, we have

$$\tilde{\mu}(x_2) - \tilde{\mu}(x_1) = -J \int_{x_1}^{x_2} dx \, \frac{1}{\sigma(\rho(x))} \tag{B.12}$$

for any x_1 and x_2. Even though $\sigma(\rho(\hat{x}))$ is discontinuous at $\hat{x} = X$, the integration in the right-side of (B.12) gives a continuous function in x_2 and x_1. Thus, $\tilde{\mu}(\hat{x})$ is a continuous function in the limit $L \to \infty$.

Here, the key idea for the determination of $\mu(\hat{x} = X)$ is the introduction of the generalized pressure $\tilde{p}$ satisfying

$$\rho \partial_x \tilde{\mu} = \partial_x \tilde{p}. \tag{B.13}$$

We can explicitly derive $\tilde{p}$ from (B.11) and (B.13) as

$$\tilde{p} = p(\rho) - \kappa \rho \partial_x^2 \rho + \frac{\kappa}{2} (\partial_x \rho)^2, \tag{B.14}$$

which was first obtained by van der Waals [29]. By integrating (B.13) in the range $[x_1, x_2]$, we have

$$\tilde{p}(x_2) - \tilde{p}(x_1) = -J \int_{x_1}^{x_2} dx \, \frac{\rho(x)}{\sigma(\rho(x))}, \tag{B.15}$$

for any x_1 and x_2. We find from (B.15) that $\tilde{p}(\hat{x})$ is a continuous function in the limit $L \to \infty$. Note that $\tilde{p}(x) = p_{\mathrm{c}}$ for the equilibrium system, where p_{c} is the constant given in (B.3).

Now, using the continuity of $\tilde{\mu}(\hat{x})$ and $\tilde{p}(\hat{x})$ at $\hat{x} = X$, we can determine the values of $\rho(\hat{x} = X - \epsilon)$ and $\rho(\hat{x} = X + \epsilon)$ for small $\epsilon > 0$ in the limit $L \to \infty$. Let ρ_- and ρ_+ be $\rho(\hat{x} = X - \epsilon)$ and $\rho(\hat{x} = X - \epsilon)$ for $\epsilon \to 0+$ after taking the limit $L \to \infty$. The continuity of $\tilde{\mu}(\hat{x})$ and $\tilde{p}(\hat{x})$ at $\hat{x} = X$ leads to

$$\mu(\rho_-) = \mu(\rho_+), \qquad p(\rho_-) = p(\rho_+). \tag{B.16}$$

Recalling (B.8), we obtain

$$\rho_- = \rho_{\mathrm{c}}^{\mathrm{L}}, \qquad \rho_+ = \rho_{\mathrm{c}}^{\mathrm{G}}. \tag{B.17}$$

Therefore, the chemical potential at the interface is equal to μ_{c}. The result is mentioned in the third paragraph of Sect. 2.3 in the main text.

Finally, we present a remark on the singular continuum description for the case $\kappa_\Lambda \to 0$ in Sect. 2.4. The chemical potential $\mu(\hat{x})$ is continuous at the interface position $\hat{x} = X$ where $\rho(\hat{x})$ is discontinuous. In this case, however, $p(\hat{x})$ is discontinuous at $\hat{x} = X$, as shown by (4.27). That is, (B.13) does not hold at the interface. This is the most essential difference between the two cases $\kappa_\Lambda \gg 1$ and $\kappa_\Lambda \ll 1$.

Appendix C: Zubarev-McLennan Representation

In this section, we derive the Zubarev-McLennan representation (3.1) in Sect. 3.1.

We study stochastic processes of $\boldsymbol{\psi} = (\psi_i)_{1\le i\le N}$ defined by (A.1). The time evolution of $\boldsymbol{\psi}$ is described by (A.4). Let $\hat{\boldsymbol{\psi}} = (\boldsymbol{\psi}_t)_{t=0}^{\tau}$ be a trajectory in the time interval $[0, \tau]$. The path probability density $\mathcal{P}_{\mathrm{path}}(\hat{\boldsymbol{\psi}})$ in the system with $\phi > 0$ starting from a density profile sampled from an equilibrium distribution $\mathcal{P}_{\mathrm{eq}}(\boldsymbol{\psi}_0)$ is expressed as

$$\begin{aligned}\mathcal{P}_{\mathrm{path}}(\hat{\boldsymbol{\psi}}) &= \mathcal{P}_{\mathrm{eq}}(\boldsymbol{\psi}_0) \times \text{const} \\ &\times \exp\left(-\frac{1}{4T_{\mathrm{eff}}}\int_0^\tau dt \sum_{i=1}^{N} \frac{\Lambda}{\sigma(\rho_i^{\mathrm{m}})}\left[\frac{d\psi_i}{dt} + \frac{\sigma(\rho_i^{\mathrm{m}})}{\Lambda}\left(\frac{\partial \mathcal{F}}{\partial \psi_i} + \phi\delta_{i,N}\right)\right]^2\right).\end{aligned} \tag{C.1}$$

For the time-reversed trajectory $\hat{\boldsymbol{\psi}}^\dagger = (\boldsymbol{\psi}_{\tau-t})_{t=0}^{\tau}$ of $\hat{\boldsymbol{\psi}}$, we have

$$\begin{aligned}\mathcal{P}_{\mathrm{path}}(\hat{\boldsymbol{\psi}}^\dagger) &= \mathcal{P}_{\mathrm{eq}}(\boldsymbol{\psi}_\tau) \times \text{const} \\ &\times \exp\left(-\frac{1}{4T_{\mathrm{eff}}}\int_0^\tau dt \sum_{i=1}^{N} \frac{\Lambda}{\sigma(\rho_i^{\mathrm{m}})}\left[-\frac{d\psi_i}{dt} + \frac{\sigma(\rho_i^{\mathrm{m}})}{\Lambda}\left(\frac{\partial \mathcal{F}}{\partial \psi_i} + \phi\delta_{i,N}\right)\right]^2\right).\end{aligned} \tag{C.2}$$

The ratio of the two yields

$$\frac{\mathcal{P}_{\mathrm{path}}(\hat{\boldsymbol{\psi}})}{\mathcal{P}_{\mathrm{path}}(\hat{\boldsymbol{\psi}}^\dagger)} = \exp\left[-\frac{1}{T_{\mathrm{eff}}}\phi\int_0^\tau dt \frac{d\psi_N(t)}{dt}\right], \tag{C.3}$$

where (A.6) has been substituted into $\mathcal{P}_{\mathrm{eq}}(\boldsymbol{\psi}_0)$ and $\mathcal{P}_{\mathrm{eq}}(\boldsymbol{\psi}_\tau)$.

To simplify the notation, we introduce the accumulated current

$$Q_\tau(\hat{\boldsymbol{\psi}}) \equiv \int_0^\tau dt\ j_N(t). \tag{C.4}$$

Using (A.1) and (C.4), we rewrite (C.3) as

$$\frac{\mathcal{P}_{\mathrm{path}}(\hat{\boldsymbol{\psi}})}{\mathcal{P}_{\mathrm{path}}(\hat{\boldsymbol{\psi}}^\dagger)} = \exp\left[\frac{\phi Q_\tau}{T_{\mathrm{eff}}}\right]. \tag{C.5}$$

The distribution of $\boldsymbol{\psi}$ at time t is expressed as

$$\begin{aligned}\mathcal{P}_\tau(\boldsymbol{\psi}) &= \int \mathcal{D}\hat{\boldsymbol{\psi}}\ \mathcal{P}_{\text{path}}(\hat{\boldsymbol{\psi}})\delta(\boldsymbol{\psi}_\tau - \boldsymbol{\psi}) \\ &= \int \mathcal{D}\hat{\boldsymbol{\psi}}^\dagger \exp\left[\frac{\phi Q_\tau(\hat{\boldsymbol{\psi}})}{T_{\text{eff}}}\right]\mathcal{P}_{\text{path}}(\hat{\boldsymbol{\psi}}^\dagger)\delta(\boldsymbol{\psi}_\tau - \boldsymbol{\psi}),\end{aligned} \tag{C.6}$$

where we have used $\mathcal{D}\hat{\boldsymbol{\psi}} = \mathcal{D}\hat{\boldsymbol{\psi}}^\dagger$ and (C.5). When the path integration variable is transformed, the right side of (C.6) is rewritten as

$$\begin{aligned}&\int \mathcal{D}\hat{\boldsymbol{\psi}}\ \exp\left[\frac{\phi Q_\tau(\hat{\boldsymbol{\psi}}^\dagger)}{T_{\text{eff}}}\right]\mathcal{P}_{\text{path}}(\hat{\boldsymbol{\psi}})\delta(\boldsymbol{\psi}_0 - \boldsymbol{\psi}), \\ &= \int \mathcal{D}\hat{\boldsymbol{\psi}}\ \exp\left[-\frac{\phi Q_\tau(\hat{\boldsymbol{\psi}})}{T_{\text{eff}}}\right]\mathcal{P}_{\text{path}}(\hat{\boldsymbol{\psi}})\delta(\boldsymbol{\psi}_0 - \boldsymbol{\psi}),\end{aligned} \tag{C.7}$$

where we have used $Q_\tau(\hat{\boldsymbol{\psi}}^\dagger) = -Q_\tau(\hat{\boldsymbol{\psi}})$. We thus have the relation

$$\mathcal{P}_\tau(\boldsymbol{\psi}) = \mathcal{P}_{\text{eq}}(\boldsymbol{\psi})\left\langle \exp\left[-\frac{\phi Q_\tau}{T_{\text{eff}}}\right]\right\rangle_{\boldsymbol{\psi}}. \tag{C.8}$$

Taking the limit $\tau \to \infty$, we have

$$\mathcal{P}_{\text{ss}}(\boldsymbol{\psi}) = \mathcal{P}_{\text{eq}}(\boldsymbol{\psi})\left\langle \exp\left[-\frac{\phi Q}{T_{\text{eff}}}\right]\right\rangle_{\boldsymbol{\psi}} \tag{C.9}$$

with

$$Q = \int_0^\infty dt\ j_N(t). \tag{C.10}$$

In the limit $T_{\text{eff}} \to 0$, we estimate

$$\left\langle \exp\left[-\frac{\phi Q}{T_{\text{eff}}}\right]\right\rangle_{\boldsymbol{\psi}} \simeq \exp\left[-\frac{\phi \langle Q\rangle_{\boldsymbol{\psi}}}{T_{\text{eff}}}\right]. \tag{C.11}$$

We then expand $\langle Q\rangle_{\boldsymbol{\psi}}$ in ϕ, and we obtain

$$\mathcal{P}_{\text{ss}}(\boldsymbol{\psi}) = \mathcal{P}_{\text{eq}}(\boldsymbol{\psi})\exp\left[-\frac{\phi \langle Q\rangle_{\boldsymbol{\psi}}^{\text{eq}} + O(\phi^2)}{T_{\text{eff}}}\right]. \tag{C.12}$$

This is the Zubarev-McLennan representation of the steady state distribution. By using (A.2), we obtain the stationary distribution of $\boldsymbol{\rho}$ as the form (3.1).

Appendix D: Derivation of (3.23)

In (3.21), we consider the decomposition of $j(0,t)$ into $\Phi(t)$ and $\Phi_0(t)$. In this section, we calculate $\Phi_0(t)$.

D.1: Preliminaries for the Calculation

We first note that (3.14) and (3.16) yield

$$\frac{d\hat{X}_\downarrow}{dt} = \frac{d\hat{Y}}{dt} + \frac{1}{2}\frac{d|D^{\mathrm{L}}|}{dt}, \qquad \frac{d\hat{X}_\uparrow}{dt} = \frac{d\hat{Y}}{dt} - \frac{1}{2}\frac{d|D^{\mathrm{L}}|}{dt}, \qquad \frac{d|D^{\mathrm{G}}|}{dt} = -\frac{d|D^{\mathrm{L}}|}{dt}. \tag{D.1}$$

From the chain rule of the derivative, we have

$$\begin{aligned}\frac{d}{dt}\left[\frac{|D^{\mathrm{L}}|}{\sigma^{\mathrm{L}}} + \frac{|D^{\mathrm{G}}|}{\sigma^{\mathrm{G}}}\right]^{-1} &= -\left[\frac{|D^{\mathrm{L}}|}{\sigma^{\mathrm{L}}} + \frac{|D^{\mathrm{G}}|}{\sigma^{\mathrm{G}}}\right]^{-2} \circ \left[\frac{1}{\sigma^{\mathrm{L}}}\frac{d|D^{\mathrm{L}}|}{dt} + \frac{1}{\sigma^{\mathrm{G}}}\frac{d|D^{\mathrm{G}}|}{dt}\right] \\ &= -\left(\frac{1}{\sigma^{\mathrm{L}}} - \frac{1}{\sigma^{\mathrm{G}}}\right)\left[\frac{|D^{\mathrm{L}}|}{\sigma^{\mathrm{L}}} + \frac{|D^{\mathrm{G}}|}{\sigma^{\mathrm{G}}}\right]^{-2} \circ \frac{d|D^{\mathrm{L}}|}{dt},\end{aligned} \tag{D.2}$$

and

$$\begin{aligned}&\frac{d}{dt}\left[\frac{1}{\sigma^{\mathrm{L}}}\int_{D^{\mathrm{L}}} dx\, \psi + \frac{1}{\sigma^{\mathrm{G}}}\int_{D^{\mathrm{G}}} dx\, \psi\right] = \frac{d}{dt}\left[\frac{1}{\sigma^{\mathrm{L}}}\int_{\hat{X}_\uparrow(t)}^{\hat{X}_\downarrow(t)} dx\, \psi + \frac{1}{\sigma^{\mathrm{G}}}\int_{\hat{X}_\downarrow(t)}^{\hat{X}_\uparrow(t)+1} dx\, \psi\right] \\ &= \frac{1}{\sigma^{\mathrm{L}}}\left[\psi(\hat{X}_\downarrow(t), t) \circ \frac{d\hat{X}_\downarrow}{dt} - \psi(\hat{X}_\uparrow(t), t) \circ \frac{d\hat{X}_\uparrow}{dt}\right] \\ &\quad + \frac{1}{\sigma^{\mathrm{G}}}\left[\psi(\hat{X}_\uparrow(t), t) \circ \frac{d\hat{X}_\uparrow}{dt} - \psi(\hat{X}_\downarrow(t), t) \circ \frac{d\hat{X}_\downarrow}{dt}\right] \\ &\quad + \frac{1}{\sigma^{\mathrm{L}}}\int_{D^{\mathrm{L}}} dx\, \partial_t\psi + \frac{1}{\sigma^{\mathrm{G}}}\int_{D^{\mathrm{G}}} dx\, \partial_t\psi \\ &= \left(\frac{1}{\sigma^{\mathrm{L}}} - \frac{1}{\sigma^{\mathrm{G}}}\right)\left[\left(\psi(\hat{X}_\downarrow(t), t) - \psi(\hat{X}_\uparrow(t), t)\right) \circ \frac{d\hat{Y}}{dt}\right. \\ &\quad \left. + \frac{1}{2}\left(\psi(\hat{X}_\downarrow(t), t) + \psi(\hat{X}_\uparrow(t), t)\right) \circ \frac{d|D^{\mathrm{L}}|}{dt}\right] \\ &\quad + \frac{1}{\sigma^{\mathrm{L}}}\int_{D^{\mathrm{L}}} dx\, \partial_t\psi + \frac{1}{\sigma^{\mathrm{G}}}\int_{D^{\mathrm{G}}} dx\, \partial_t\psi.\end{aligned} \tag{D.3}$$

D.2: Relation Between $\Phi(t)$ and $j(0, t)$

Noting the two derivatives (D.2) and (D.3), we define

$$\Phi_1 \equiv -\left(\frac{1}{\sigma^{\mathrm{L}}} - \frac{1}{\sigma^{\mathrm{G}}}\right)\left[\frac{|D^{\mathrm{L}}|}{\sigma^{\mathrm{L}}} + \frac{|D^{\mathrm{G}}|}{\sigma^{\mathrm{G}}}\right]^{-2}\left[\frac{1}{\sigma^{\mathrm{L}}}\int_{D^{\mathrm{L}}(t)} dx\, \psi + \frac{1}{\sigma^{\mathrm{G}}}\int_{D^{\mathrm{G}}(t)} dx\, \psi\right] \circ \frac{d|D^{\mathrm{L}}|}{dt}, \tag{D.4}$$

$$\begin{aligned}\Phi_2 \equiv &\left(\frac{1}{\sigma^{\mathrm{L}}} - \frac{1}{\sigma^{\mathrm{G}}}\right)\left[\frac{|D^{\mathrm{L}}|}{\sigma^{\mathrm{L}}} + \frac{|D^{\mathrm{G}}|}{\sigma^{\mathrm{G}}}\right]^{-1} \times \left[\left(\psi(\hat{X}_\downarrow(t), t) - \psi(\hat{X}_\uparrow(t), t)\right) \circ \frac{d\hat{Y}}{dt}\right. \\ &\left. + \frac{1}{2}\left(\psi(\hat{X}_\downarrow(t), t) + \psi(\hat{X}_\uparrow(t), t)\right) \circ \frac{d|D^{\mathrm{L}}|}{dt}.\right]\end{aligned} \tag{D.5}$$

Then, the definition of $\Phi(t)$ in (3.22) leads to

$$\Phi(t) = \Phi_1(t) + \Phi_2(t) + j(0, t) \tag{D.6}$$

by using (3.20). Here, from the piece-wise linear nature of $\psi(x,t)$, we have

$$\frac{1}{\sigma^{\rm L}}\int_{D^{\rm L}(t)} dx\ \psi + \frac{1}{\sigma^{\rm G}}\int_{D^{\rm G}(t)} dx\ \psi = \frac{1}{2}\left[\frac{|D^{\rm L}|}{\sigma^{\rm L}} + \frac{|D^{\rm G}|}{\sigma^{\rm G}}\right]\left(\psi(\hat{X}_\downarrow(t),t) + \psi(\hat{X}_\uparrow(t),t)\right). \tag{D.7}$$

See also (3.31) for the same equation. Using this relation, we obtain

$$\Phi_1 + \Phi_2 = \left(\frac{1}{\sigma^{\rm L}} - \frac{1}{\sigma^{\rm G}}\right)\left[\frac{|D^{\rm L}(t)|}{\sigma^{\rm L}} + \frac{|D^{\rm G}(t)|}{\sigma^{\rm G}}\right]^{-1}\left(\psi(\hat{X}_\downarrow(t),t) - \psi(\hat{X}_\uparrow(t),t)\right)\circ\frac{d\hat{Y}}{dt}. \tag{D.8}$$

Finally, we note that

$$\begin{aligned}\psi(\hat{X}_\downarrow(t),t) - \psi(\hat{X}_\uparrow(t),t) &= \int_{D^{\rm L}} dx\ \partial_x\psi,\\ &= |D^{\rm L}(t)|(\rho^{\rm L}(t) - \bar{\rho}).\end{aligned} \tag{D.9}$$

Substituting this into (D.8), we obtain (3.23) where $\Phi_0 \equiv \Phi_1 + \Phi_2$.

Acknowledgements The authors thank F. Kagawa, K. Saito, and Y. Yamamura for useful discussions about experiments on non-equilibrium phase coexistence; M. Kobayashi, S. Yukawa, and A. Yoshida for discussions on numerical simulations of non-equilibrium phase coexistence; and K. Hiura, M. Itami, H. Nakano and Y. Nakayama for discussions on fluctuating hydrodynamics. We also thank B. Derrida, C. Maes, H. Spohn, and H. Tasaki for suggesting us to study boundary-driven diffusive systems. This work was supported by JSPS KAKENHI Grant Number JP22H01144 and JP23K22415.

Data Availability Data sharing not applicable to this article as no datasets were generated or analysed during the current study.

Declarations

Conflict of interest The authors have no financial or proprietary interests in any material discussed in this article.

References

1. Thome, J.R.: Boiling in microchannels: a review of experiment and theory. Int. J. Heat Fluid flow **25**, 128–139 (2004)
2. Ben-Jacob, E., Garik, P.: The formation of patterns in nonequilibrium growth. Nature **343**, 523–530 (1990)
3. Ahlers, G., Berge, L.I., Cannell, D.S.: Thermal convection in the presence of a first-order phase change. Phys. Rev. Lett. **70**, 2399 (1993)
4. Yoshida, A., Nakagawa, N., Sasa, S.-I.: Heat-induced liquid hovering in liquid-gas coexistence under gravity. Phys. Rev. Lett. **133**, 117101 (2024)
5. Zhong, J.-Q., Funfschilling, D., Ahlers, G.: Enhanced heat transport by turbulent two-phase Rayleigh-Benard convection. Phys. Rev. Lett. **102**, 124501 (2009)
6. Weiss, S., Ahlers, G.: Nematic-isotropic phase transition in turbulent thermal convection. J. Fluid Mech. **737**, 308–328 (2013)

7. Urbana, P., Schmoranzerb, D., Hanzelkaa, P., Sreenivasanc, K.R., Skrbekb, L.: Anomalous heat transport and condensation in convection of cryogenic helium. Proc. Natl. Acad. Sci. **110**, 8036–8039 (2013)
8. Cates, M.E., Tailleur, J.: Motility-induced phase separation. Annu. Rev. Condens. Matter Phys. **6**, 219–244 (2015)
9. Nakagawa, N., Sasa, S.-I.: Liquid-gas transitions in steady heat conduction. Phys. Rev. Lett. **119**, 260602 (2017)
10. Nakagawa, N., Sasa, S.-I.: Global thermodynamics for heat conduction states. J. Stat. Phys. **177**, 825–888 (2019)
11. Nakagawa, N., Sasa, S.-I.: Unique extension of the maximum entropy principle to phase coexistence in heat conduction. Phys. Rev. Res. **4**, 033155 (2022)
12. Kobayashi, M., Nakagawa, N., Sasa, S.-I.: Control of metastable states by heat flux in the Hamiltonian Potts model. Phys. Rev. Lett. **130**, 247102 (2023)
13. Sasa, S.-I., Nakagawa, N., Itami, M., Nakayama, Y.: Stochastic order parameter dynamics for phase coexistence in heat conduction. Phys. Rev. E **103**, 062129 (2021)
14. Schmitz, R.: Fluctuations in nonequilibrium fluids. Phys. Rep. **171**, 1–58 (1988)
15. Eyink, G.L.: Dissipation and large thermodynamic fluctuations. J. Stat. Phys. **61**, 533–572 (1990)
16. Spohn, H.: Large scale dynamics of interacting particles. Springer-Verlag, Berlin/Heidelberg (1991)
17. Bertini, L., De Sole, A., Gabrielli, D., Jona-Lasinio, G., Landim, C.: Macroscopic fluctuation theory. Rev. Mod. Phys. **87**, 593 (2015)
18. Kuramoto, Y.: Effects of diffusion on the fluctuations in open chemical systems. Prog. Theor. Phys. **52**, 711 (1974)
19. Yanagisawa, Y., Sasa, S.-i.: Phase coexistence in a weakly stochastic reaction-diffusion system. Phys. Rev. E **111**, L012103 (2025)
20. Kado, Y., Sasa, S.-I.: Microscopic singularity of an entropic force in stochastic order parameter dynamics. Phys. Rev. Lett. **132**, 057101 (2024)
21. Zubarev, D.N.: Nonequilibrium Statistical Thermodynamics. Consultants Bureau, New York (1974)
22. McLennan, J.A.: Statistical mechanics of transport in fluids. Phys. Fluids **3**, 493 (1960)
23. McLennan, J.A.: Introduction to Non-equilibrium Statistical Mechanics. Prentice-Hall, Hoboken (1988)
24. Crooks, G.E.: Path-ensemble averages in systems driven far from equilibrium. Phys. Rev. E **61**, 2361 (2000)
25. Sasa, S.-I.: A perturbation theory for large deviation functionals in fluctuating hydrodynamics. J. Phys. A **41**, 045006 (2008)
26. Komatsu, T.S., Nakagawa, N.: Expression for the stationary distribution in nonequilibrium steady states. Phys. Rev. Lett. **100**, 030601 (2008)
27. Maes, C., Netočný, K.: Rigorous meaning of McLennan ensembles. J. Math. Phys. **51**, 015219 (2010)
28. Nakagawa, N., Sasa, S.-I., Hirao, T., Shiina, T., Tachi, K., Yoshida, A.: Global thermodynamics for isothermal fluids under gravity. arXiv:2412.19643 (2024)
29. Rowlinson, J.S.: Translation of J. D. van der Waals' "The thermodynamik theory of capillarity under the hypothesis of a continuous variation of density". J. Stat. Phys. **20**, 197 (1979)